Enhancing the brain's emotion regulation capacity with a randomised trial of a 5-week heart rate variability biofeedback intervention

Kaoru Nashiro[1], Jungwon Min[1], Hyun Joo Yoo[1], Christine Cho[1], Shelby L. Bachman[1], Shubir Dutt[1], Julian F. Thayer[2], Paul Lehrer[3], Tiantian Feng[1], Noah Mercer[1], Padideh Nasseri[1], Diana Wang[1], Catie Chang[4], Vasilis Z. Marmarelis[1], Shri Narayanan[1], Daniel A. Nation[2], and Mara Mather[1]*

[1]University of Southern California, [2]University of California, Irvine, [3]Rutgers University, [4]Vanderbilt University

Kaoru Nashiro, Ph.D.
Research Assistant Professor
Leonard Davis School of Gerontology
University of Southern California
nashiro@usc.edu

Jungwon Min
Graduate Student
Department of Psychology
Dornsife College of Letters, Arts and Sciences
University of Southern California
minjungw@usc.edu

Hyun Joo Yoo, Ph.D.
Research Associate
Leonard Davis School of Gerontology
University of Southern California
hyunjooy@usc.edu

Christine Cho
Project Manager
Leonard Davis School of Gerontology
University of Southern California
cho890@usc.edu

Shelby L. Bachman
Graduate Student
Leonard Davis School of Gerontology
University of Southern California
sbachman@usc.edu

Shubir Dutt
Graduate Student
Department of Psychology
Dornsife College of Letters, Arts and Sciences
University of Southern California
shubirdu@usc.edu

Julian F. Thayer, Ph.D.
Professor
Department of Psychological Science
University of California, Irvine
jfthayer@uci.edu

Paul Lehrer, Ph.D.
Professor
Department of Psychiatry
Rutgers University
lehrer@rwjms.rutgers.edu

Tiantian Feng
Graduate Student
Department of Computer Science
Viterbi School of Engineering
University of Southern California
tiantiaf@usc.edu

Noah Mercer
Software Consultant

noahmerc@usc.edu

Padideh Nasseri
Graduate Student
Neuroscience Graduate Program
University of Southern California
pnasseri@usc.edu

Diana Wang, Ph.D.
Postdoctoral Research Scholar
Center for Economic and Social Research
Dornsife College of Letters, Arts and Sciences
University of Southern California
diana.wang.1@usc.edu

Catie Chang, Ph.D.
Assistant Professor
Departments of Computer Science, Electrical Engineering, Computer Engineering and Biomedical Engineering
School of Engineering
Vanderbilt University
catie.chang@vanderbilt.edu

Vasilis Z. Marmarelis, Ph.D.
Professor
Department of Biomedical Engineering
Viterbi School of Engineering
University of Southern California
vzm@usc.edu

Shri Narayanan, Ph.D.
Professor
Departments of Electrical & Computer Engineering and Computer Science
Viterbi School of Engineering
University of Southern California
shri@ee.usc.edu

Daniel A. Nation, Ph.D.
Associate Professor
Department of Psychological Science
University of California, Irvine
dnation@uci.edu

Mara Mather, Ph.D.
Professor
Leonard Davis School of Gerontology
University of Southern California
mara.mather@usc.edu

Abstract

Heart rate variability is a robust biomarker of emotional well-being, consistent with the shared brain networks regulating emotion regulation and heart rate. While high heart rate oscillatory activity clearly indicates healthy regulatory brain systems, can increasing this oscillatory activity also enhance brain function? To test this possibility, we randomly assigned 106 young adult participants to one of two 5-week interventions involving daily biofeedback that either increased heart rate oscillations (Osc+ condition) or had little effect on heart rate oscillations (Osc- condition) and examined effects on brain activity during rest and during regulating emotion. In this healthy cohort, the two conditions did not differentially affect anxiety, depression or mood. However, the Osc+ intervention increased low-frequency heart rate variability and increased brain oscillatory dynamics and functional connectivity in emotion-related resting-state networks. It also increased down-regulation of activity in somatosensory brain regions during an emotion regulation task. The Osc- intervention did not have these effects. These findings indicate that heart rate oscillatory activity not only reflects the current state of regulatory brain systems but also changes how the brain operates beyond the moments of high oscillatory activity.

People with higher heart rate variability tend to regulate their emotions more effectively[1,2]. But the variability associated with effective emotion regulation is not just random noise; instead, it is the degree to which heart rhythms synchronize with breathing. When inhaling, heart rate typically speeds up, and when exhaling, heart rate typically slows down, due to signals transmitted between the brain and the heart via the vagus nerve.

Why should having a heart rate that responds more to breathing be associated with emotion regulation? One potential explanation is that many of the same brain regions are involved in coordinating heart rhythms and in regulating emotions[3]. However, heart rate oscillations may go beyond signaling the functioning of regulatory brain regions. They may improve the brain's capacity to regulate emotion[4]. Indeed, recent findings from biofeedback studies in which people increase their own heart rate oscillatory activity suggest that episodes of high amplitude heart rate oscillations reduce stress and anxiety[5]. In the typical heart rate oscillation biofeedback intervention, people slowly breathe at around 10s/breath or 0.1 Hz while receiving feedback on how much their current heart rate is oscillating in response to their breathing during daily training sessions for a few weeks[6]. Breathing at this pace creates especially high amplitude heart rate oscillations because 0.1 Hz is a resonance frequency for the baroreflex system, which also produces oscillations in heart rate[7].

Intriguingly, ~0.1 Hz oscillations in heart rate and breathing are also seen during some meditative practices[8-10], including during reciting either a yoga mantra or the rosary Ave Maria[11]. Varied cultural practices may have converged on this resonance breathing frequency that creates high oscillations in heart rate because of its positive impact on well-being.

Why would daily time spent in a high physiological oscillatory state benefit the brain's emotion regulation ability? First consider what occurs during the experience of emotions or feelings. At each moment, the brain receives diverse input about current body states, with the vagus nerve serving as a primary conduit of visceral information[12-14]. Mapping these body states in the brain is necessary to

generate feelings[15]. But the actual body state need not be present. People can simulate body state changes in insula and somatosensory cortices, influencing current feeling states[16,17]. This system allows for top-down modulation over feelings and emotions, as prefrontal, anterior cingulate and anterior insula regions both respond to and modulate activity in brain regions mapping visceral and somatic sensations.

Cortical brain regions involved in autonomic control including the insula and ventromedial prefrontal cortex respond to increasing or decreasing heart period intervals, supporting feedback loops that control blood flow to different areas of the body, modulate heart rate, and provide rapid responses to arterial blood pressure changes. Inducing large oscillations may strengthen the ability of autonomic control processes to respond to changes in somatosensory inputs, which in turn should enhance the ability to modulate fluctuations in one's own feelings. If inducing heart rate oscillations strengthens dynamic control over emotion regulation in this way, the effects should be evident during times when the system is challenged by stimuli that induce emotions. These same feedback loops likely contribute to resting-state oscillatory activity in emotion-related brain regions. Thus, daily sessions spent in a high physiological oscillatory state may also increase the coordinated activity of emotion-related resting-state brain networks[4].

Our study (ClinicalTrials.gov NCT03458910; Heart Rate Variability and Emotion Regulation or "HRV-ER") tested the hypothesis that daily biofeedback sessions stimulating heart rate oscillatory activity in baroreflex frequencies affect the function of brain networks involved in emotion regulation, even when people are not engaged in the biofeedback. We randomly assigned 106 young adult participants to receive either 'increase-oscillations' (Osc+) or 'decrease-oscillations' (Osc-) biofeedback in daily training sessions for five weeks in a 7-week study involving pre- and post-intervention assessments (see Fig. 1 for study schedule and Supplementary Tables 1-2 and Supplementary Fig. 1 for

participant information). We also recruited an older adult cohort whose results will be reported in a subsequent paper.

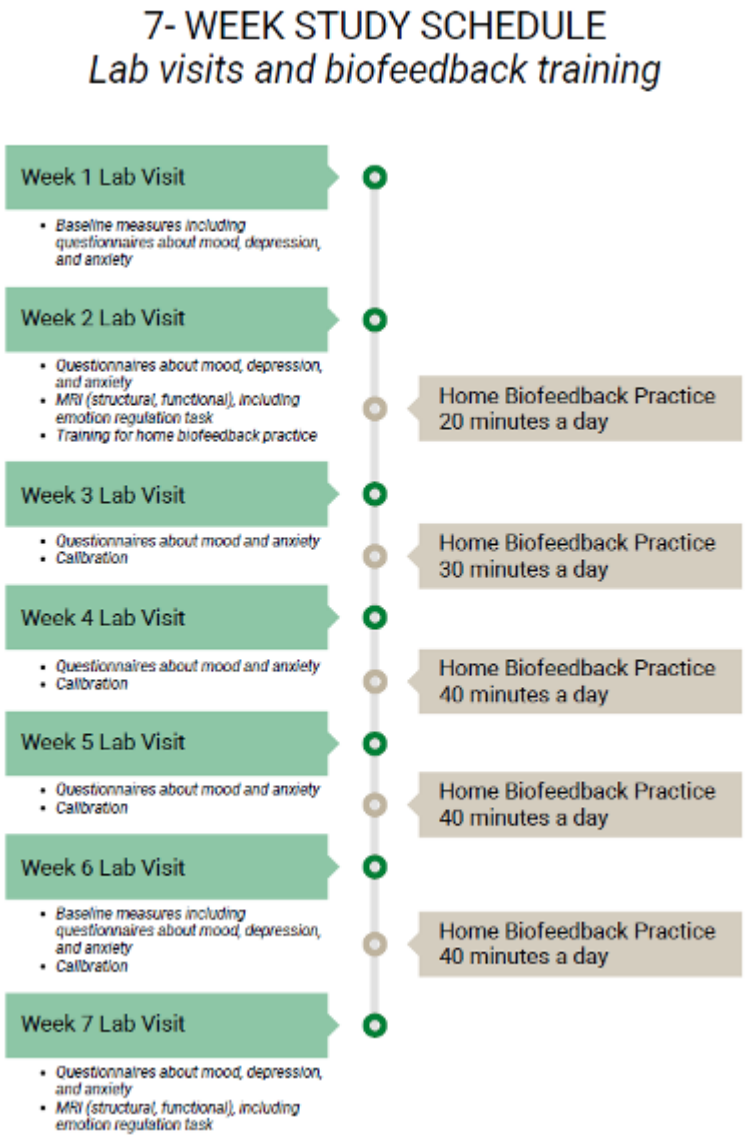

Figure 1. Overview of the schedule of weekly activities participants completed during the study.

In the Osc+ condition, participants tried out several breathing paces around 10s/breath to see which induced the largest oscillations in their heart rate (their own resonance frequency; see Methods

for details)[6]. During their daily sessions at home, they breathed to a pacer set to this frequency while receiving biofeedback on their heart rate oscillatory activity via a 'coherence' score and a real-time plot of their heart rate (Fig. 2a). They returned to the lab each week to receive coaching and check again which breathing frequency produced the strongest heart rate oscillations. Participants' assigned breathing paces ranged from 9-14s/breath.

An ideal comparison to this Osc+ intervention would be another condition with similar biofeedback information, participant expectations and time spent training but no increases in heart rate oscillatory activity during the training sessions. However, most relaxing states increase heart rate oscillations[18]. To address this, we designed a decrease-oscillations comparison condition (Osc-) in which participants received heart rate biofeedback aimed at reducing their heart rate oscillations (summarized for them with a 'calmness' score and real-time feedback on their heart rate) during the training sessions (Fig. 2b). In addition, to try to avoid having them discover that they could reduce HRV simply by increasing physical activity[19], we asked them to also try to reduce their heart rate during the training sessions. During lab sessions, they tried out different strategies to maximize their 'calmness' scores during biofeedback and were advised to use their most successful strategy in their home training sessions that week.

While we expected that, during training sessions, the Osc+ condition would increase oscillations in both heart rate and blood oxygenation level dependent (BOLD) signal at the breathing frequency significantly more than the Osc- condition, the main targets of our investigation were the more enduring effects of the biofeedback during normal breathing. We tested our hypotheses that the Osc+ intervention would affect both the connectivity of emotion networks during rest and these networks' responsiveness to acute challenges by comparing post-pre resting-state connectivity in emotion-related networks as well as brain activity during an emotion regulation task. We also examined whether

the interventions would have enduring physiological effects, influencing oscillations in heart rate and BOLD signal when participants were not training.

When preregistering our outcomes, we focused on amygdala-related effects of the intervention, due to our prior findings of relationships between amygdala functional connectivity and HRV[20] and findings that the amygdala is the primary target of emotion regulation control processes[21]. Our main outcome measure was pre-to-post intervention changes in resting-state right amygdala functional connectivity with a medial prefrontal cortex region associated with HRV[3]. As secondary emotion-related outcomes, we examined changes in up- and down-regulation of amygdala activity and self-reported emotion regulation effectiveness during viewing emotional pictures, as well as changes in ratings of emotional well-being. Secondary outcome measures also included HRV during rest and measures of cerebral blood flow. Other secondary outcome measures (e.g., decision making, stress responsivity and cognition) will be reported elsewhere. In the current report, in addition to the amygdala-focused fMRI outcomes, we also report on the broader context of how the biofeedback affected resting-state BOLD activity in canonical resting-state networks and brain activity throughout the brain during emotion regulation.

Results

Participants in the Osc+ vs. Osc- conditions (N_{Osc+} = 56; N_{Osc-} = 50) did not significantly differ in the average percent of weekly assigned session time they completed (M = 78.32%, SE = 3.43 and M = 82.74%, SE = 3.74, respectively), $t(104) = -0.87$, $p = .39$, $r = .09$, nor in their post-intervention self-rated difficulty of training, effort, expectations, or plans to continue the intervention techniques (Supplementary Fig. 2). There was also no significant effect of condition on heart rate during home training sessions, $F(1,95) = .73$, $p = .39$, $r = .09$. However, as intended, the Osc+ participants increased their heart rate total spectral frequency power during training, $t(51) = 9.26$, $p < .001$, $r = .54$; Figs. 2c and 2e), whereas the Osc- participants did not significantly influence this metric compared to their own

baseline rest (log transformed autoregressive power difference, $t(44) = 1.39$, $p = .17$, $r = .11$; Figs. 2d and 2f), leading to a significant interaction of session type (baseline vs. training) and condition, $F(1,95) = 30.37$, $p < .001$, $r = .49$. In the resonance breathing frequency range (8-16s; .063 Hz~0.125 Hz), the two conditions showed even larger differences in power during training, $F(1,95) = 43.45$, $p < .001$, $r = .56$. Prior research using sympathetic versus parasympathetic blockade indicate that such increases in spectral power during slow-paced breathing are almost entirely vagally mediated[22].

The intervention also affected resting heart rate variability. Examination of heart rate during rest revealed a significant interaction effect between time-point (pre- vs post-intervention) and condition on total power, $F(1,95) = 6.48$, $p = .01$, $r = .25$, as well as when examining just the resonance frequency range, $F(1,95) = 9.03$, $p = .003$, $r = .30$ (Figs. 2g-h). Within the resonance frequency range, the Osc+ participants had greater power after than before the intervention, $t(51) = 2.50$, $p = .02$, $r = .18$, whereas the Osc- participants had a non-significant decrease in power in that range, $t(44) = -1.79$, $p = .08$, $r = .18$. Consistent with this, as shown in Supplementary Fig. 3 and detailed in the Supplementary Information, low frequency (LF) HRV (0.04-0.15 Hz, a range covering resonance breathing frequencies and the range showing spectral power changes in Fig. 2g) showed a significant interaction of condition and time-point; the Osc+ group showed a marginally significant increase in LF-HRV from pre- to post-intervention whereas the Osc- group showed a non-significant decrease in LF-HRV. Heart rate and measures reflecting high frequency HRV showed no significant condition differences in change across the study (see Supplementary Fig. 3). Studies comparing sympathetic and parasympathetic blockade during rest indicate that nearly all of the HRV components, including LF-HRV, are predominantly under vagal control[23], thus the low frequency changes likely reflect differential changes in vagal activity during rest in the two intervention conditions.

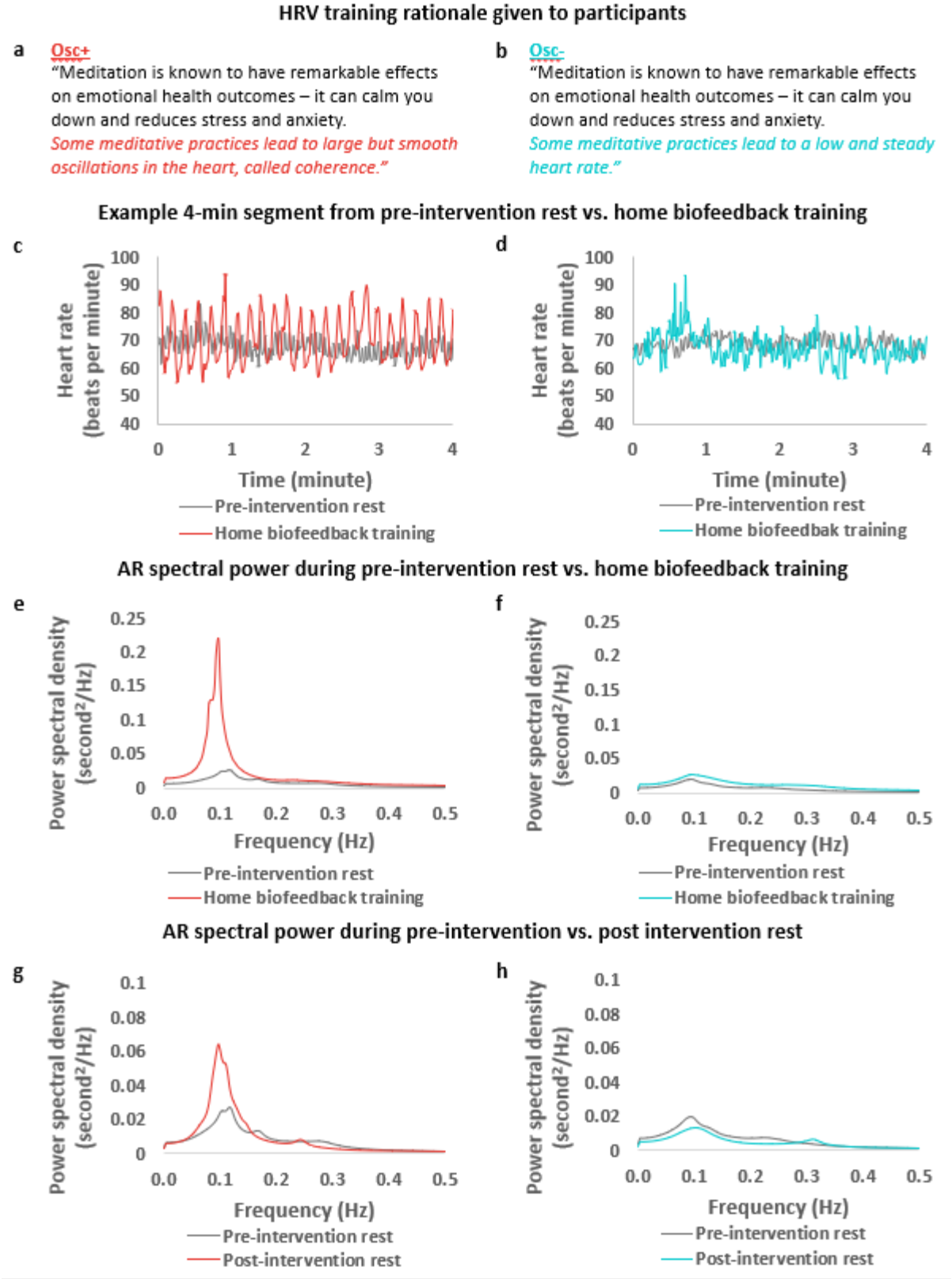

Figure 2. Comparisons of heart rate oscillatory activity during pre-intervention rest vs. training sessions in the two conditions. *a-b: Participants received similar motivating background explanations for both conditions; c-d: Example heart rate over time during pre-intervention rest vs. home biofeedback training for an Osc+ (c) vs. an Osc- participant (d); E-F: Autoregressive (AR) spectrum shows large within-condition differences between heart rate oscillatory power during pre-intervention rest vs. home biofeedback training, for Osc+ condition (e) but not Osc- (f) condition; g-h: Comparisons of heart rate oscillatory activity during rest before and after the 5-week intervention showed a significant interaction effect between time-point (pre-intervention vs post-intervention) and condition on total power. Note that pre-intervention and post-intervention resting-state heart rate was measured in single sessions in the lab (participant N = 97) whereas training data in e-f was averaged across many sessions in participants' homes (training session N = 5437).*

We examined BOLD oscillatory dynamics during resting-state scans conducted pre- and post-intervention as well as when engaging in their biofeedback technique during a "training-mimicking" post-intervention scan (see Table 1). During training-mimicking scans, participants in the Osc+ condition showed significantly greater spectral frequency total power than those in the Osc- condition, $t(81) = 4.79$, $p < .001$, $r = .47$ (Fig. 3a). Those in the Osc+ condition showed significantly greater power from pre-intervention rest to training, $t(42) = 6.09$, $p < .001$, $r = .48$, whereas those in the Osc- condition did not, $t(39) = 0.50$, $p = .62$, $r = .05$ (Fig. 3a). Grouping Osc+ participants by their instructed paced breathing rates during the training-mimicking scans shows a clear relationship between the pace at which they breathed and their BOLD oscillation peak (Fig. 3b).

The training-mimicking scan was at the end of the post-intervention scan session to avoid influencing physiology during the rest of the scans, during which participants breathed naturally. Indeed, there was not a significant time-point (Weeks 2 and 7) by condition interaction of breathing

rates during the resting-state fMRI scan, nor during the emotion-regulation task (see Supplementary Table 3 for means and statistical comparisons). In addition, during these two resting-state scans, neither exhaled carbon dioxide (CO_2) levels nor the average variability in CO_2 for the duration of the scan showed significant time-point by condition interactions. In contrast, as expected, breathing frequency and CO_2 variability differed by condition during the training-mimicking scan (see Supplementary Table 3 for means and statistical comparisons). Likewise, a 2 (time-point: pre, post) X 2 (condition: Osc+, Osc-) ANOVA on whole-brain cerebral blood flow (CBF) during pseudo-continuous arterial spin labeling (pCASL) resting-state scans showed no significant effects, whereas a 2 (scan type: pre-intervention rest, post-intervention training mimicking) X 2 (condition: Osc+, Osc-) ANOVA yielded a significant main effect of scan type, $F(1,51) = 9.48$, $p = .003$, $r = .40$, as CBF was lower during training mimicking ($M = 39.33$, $SE = 1.08$, $SD = 7.88$) than during rest ($M = 42.45$, $SE = 1.14$, $SD = 8.32$) across conditions. There was no significant main effect of condition, $F(1,51) = .91$, $p = .35$, $r = .14$, and the interaction of scan type and condition was not significant, $F(1,51) = 1.30$, $p = .26$, $r = .17$. Thus, in summary, although there were changes in breathing, CO_2, and blood flow during training-mimicking protocols, pre- and post-intervention resting states did not differ significantly on these metrics.

Comparing the average BOLD spectral frequency power across the brain during pre- vs. post-intervention rest revealed a significant interaction of condition by time-point, $F(1,92) = 5.94$, $p = .02$, $r = .24$ (Fig. 3c). There was a significant increase in total power after the intervention in the Osc+ group, $t(47) = 3.54$, $p = .001$, $r = .16$, but not in the Osc- group, $t(45) = 0.36$, $p = .72$, $r = .02$. When we include post-pre change in resting-scan respiration rate as a covariate, the interaction of condition by time-point on total power was still significant, $F(1,81) = 6.67$, $p = .01$, $r = .28$. Thus, in addition to having dramatic effects on BOLD power during training, the Osc+ training sessions had effects on BOLD power that extended beyond the training sessions to affect resting-state activity. Analyses of amplitude of low

frequency fluctuations indicated that spectral power during rest increased across resting-state networks (see Supplementary Fig. 4 and Supplementary Results).

Table 1. Functional magnetic resonance imaging (fMRI) scans and the corresponding measures employed in this study.

Functional magnetic resonance imaging (fMRI) scan	Measures Analyzed
Pre- and Post-Intervention	
Blood oxygenation level dependent (BOLD) fMRI during rest	Spectral power (Fig. 2a-b) Resting-state networks (Fig. 4) Amplitude of low frequency fluctuations (Supplementary Fig. 4) Amygdala-mPFC functional connectivity (Fig. 5) Heart rate variability during scan Breathing during scan
Pseudo continuous arterial spin labeling (pCASL) resting-state	Whole-brain cerebral blood flow
BOLD fMRI during emotion regulation task	Whole-brain contrasts of regulation conditions (Fig. 6b-c)
Post Intervention Only	
BOLD fMRI during training-mimicking	Spectral power
pCASL during training-mimicking	Whole-brain cerebral blood flow

a

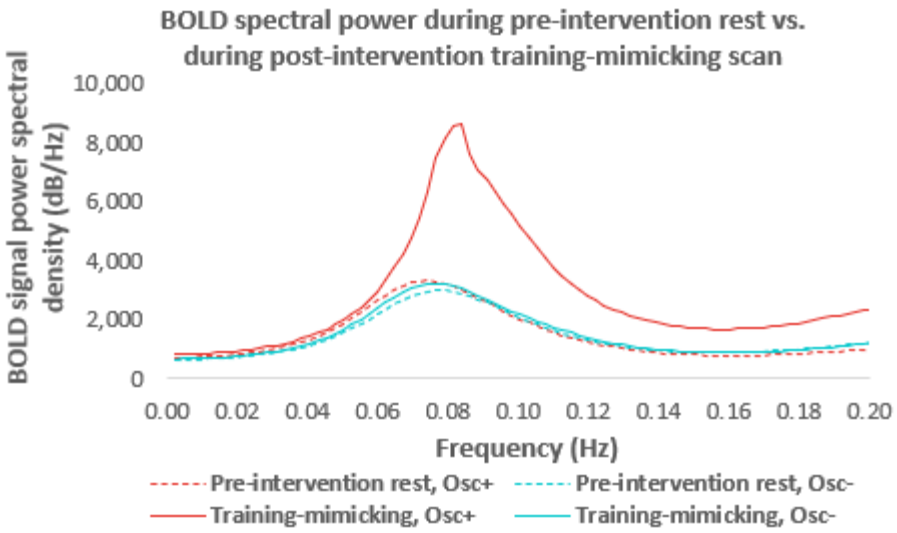

b

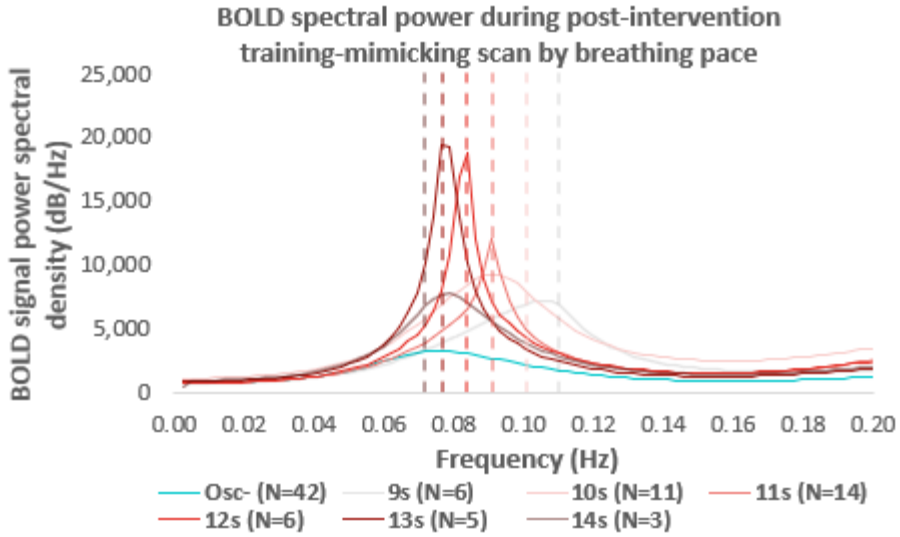

c

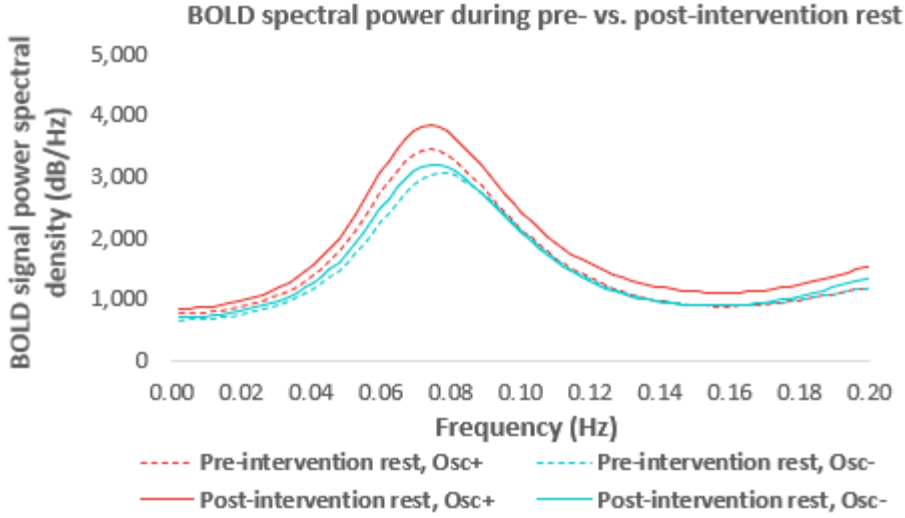

Figure 3. Blood oxygen level dependent (BOLD) autoregressive signal spectral frequency power during training and rest*. On average, Osc+ participants showed greater BOLD spectral frequency power during post-intervention training-mimicking than during pre-intervention rest session, whereas Osc- training did not significantly affect BOLD oscillatory power (a); Participants in the Osc+ condition followed breath pacers set to their own pre-determined resonance frequency (frequencies of these pacers indicated with vertical dashed lines for each subgroup of Osc+ participants) and peak BOLD power corresponded with breathing paces (b); The Osc+ but not the Osc- intervention led to increases in BOLD power during rest (c). Note that lower frequencies (<.0.04 Hz) have been removed from the spectra via a detrending procedure (see Methods).*

Quantification of functional connectivity within 18 canonical resting-state networks revealed that the two HRV biofeedback conditions also affected functional connectivity within emotion-related networks during rest. A 2 (condition: Osc+, Osc-) X 2 (network category: emotion/interoception, other; Fig. 4a) ANOVA yielded a significant interaction of condition and network category, $F(1, 94) = 5.24$, $p = .024$, $r = .23$. The Osc+ intervention increased functional connectivity within emotion-related networks significantly more than the Osc- intervention (Fig. 4b), whereas there were no significant differences between conditions for other categories of canonical resting-state networks (for breakdown of intervention effects across all 18 networks separately, see Supplementary Fig. 5).

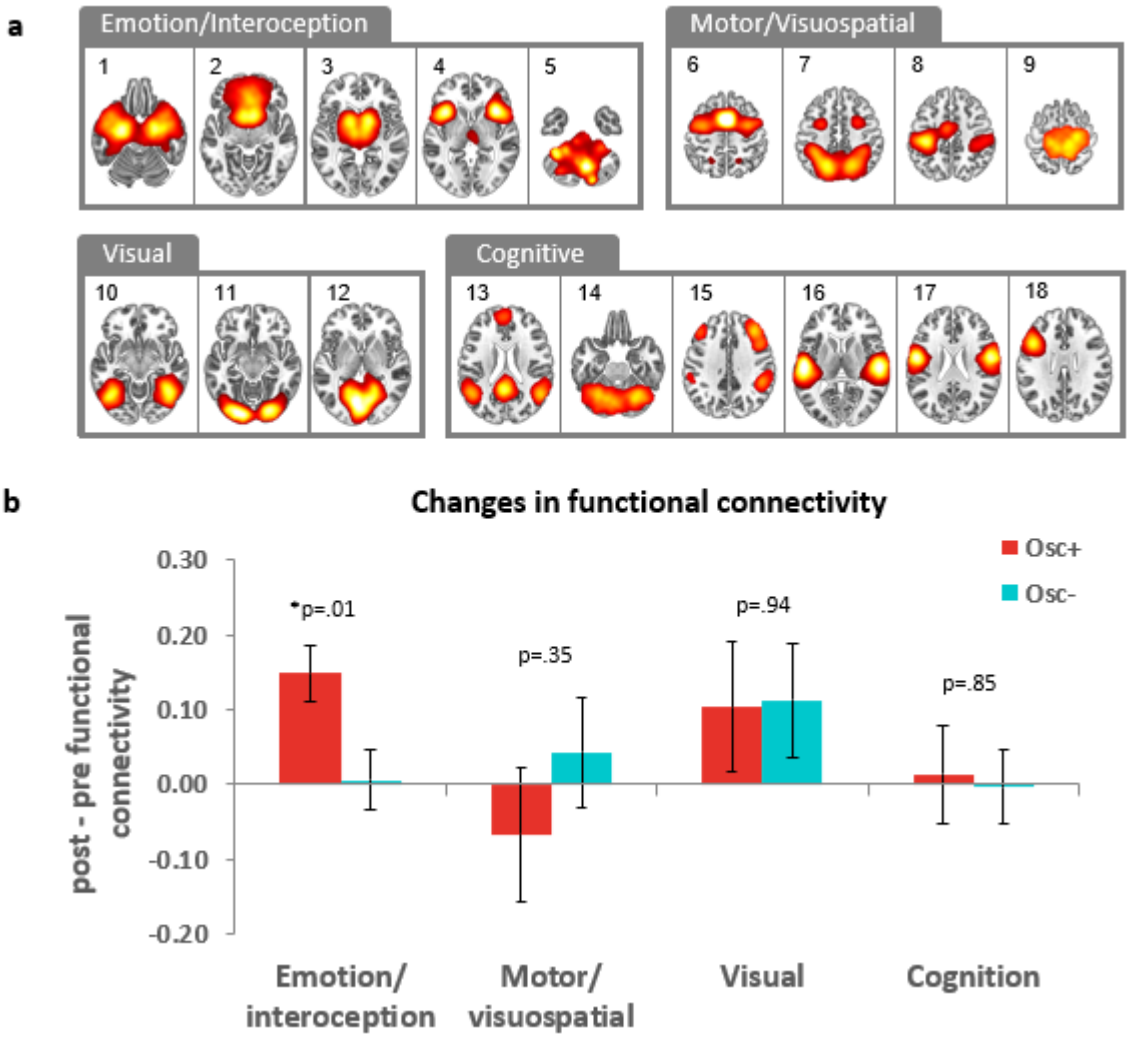

Figure 4. *We examined changes in canonical resting-state networks (a) from pre- to post-intervention resting scans; Functional connectivity within emotion-related resting state networks also increased significantly more in the Osc+ than the Osc- condition (b). *False Discovery Rate (FDR) p<.05. Error bars indicate standard error.*

Our primary outcome measure was right amygdala-medial prefrontal cortex (mPFC) functional connectivity, as this is a key emotion-related circuit[24,25] in which functional connectivity relates to individual differences in heart rate variability[20]. Seed-based analyses revealed no significant condition by time-point interaction for connectivity between mPFC and the right amygdala, $F(1, 94) = 0.68$, $p =$

.41, r = .08 (Fig. 5a), but there was a significant interaction of condition by time-point for connectivity between mPFC and the left amygdala, $F(1, 94) = 5.44$, p = .02, r = .24 (Fig. 5b), which was driven by increased connectivity in the Osc+ condition at post intervention, $t(48) = -2.33$, p = .02, r = .26.

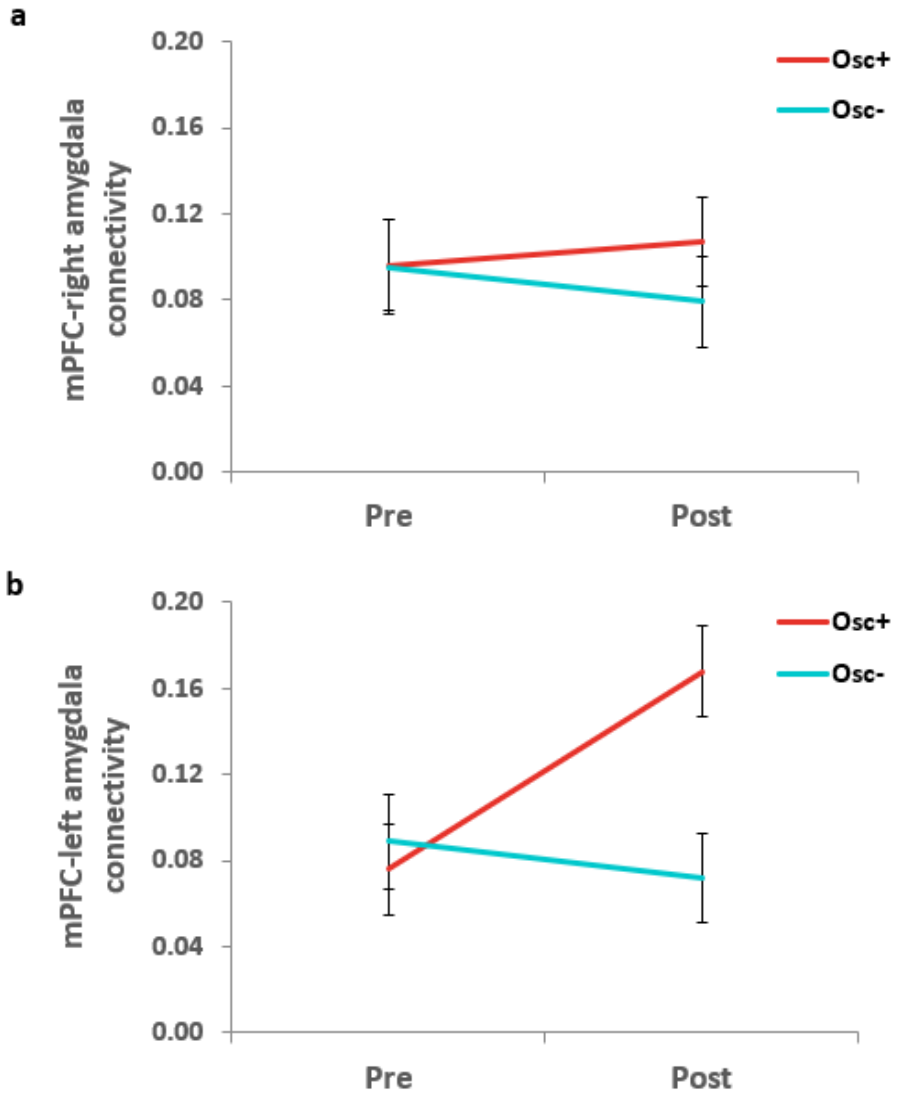

Figure 5. Functional connectivity between mPFC and amygdala during rest. *MPFC-right amygdala functional connectivity did not differ significantly by condition (a) but mPFC-left amygdala connectivity increased during the intervention in Osc+ participants more than in Osc- participants (b).*

Thus, to summarize so far, the Osc+ intervention acutely increased BOLD oscillations during the training sessions while also having longer-term effects on functional connectivity in emotion-related brain networks.

Our next question was how the intervention affected the ability to regulate brain activity associated with emotional experience during externally induced emotion. To test this, both before and after the intervention, participants completed an emotion regulation task during a functional scan of their brain. They saw negative, positive and neutral pictures one at a time. Before viewing each picture, they were asked to either intensify or diminish the emotional feelings the picture elicited, or to just view it (Fig. 6a). They were allowed to regulate emotions using strategies of their choice, but on post-task questionnaires over 95% of participants indicated relying on cognitive reappraisal strategies.

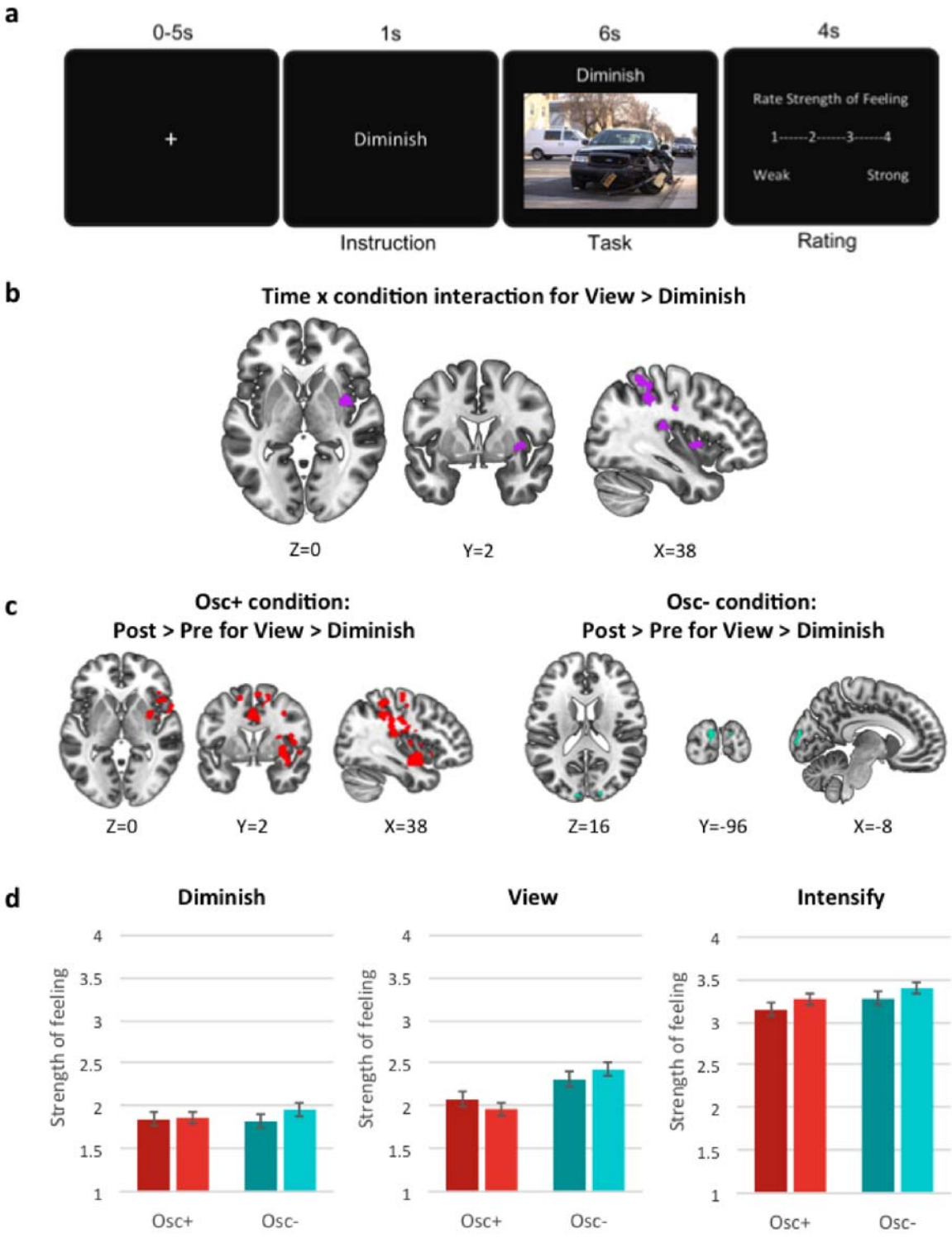

Figure 6. Trial design and results of the emotion regulation task. *After one of the three instructions (i.e., intensify, diminish or view) was given, participants viewed each picture, performed the task, and rated the*

strength of feeling (a). Brain activity during Diminish trials (relative to View) showed significant time-point-by-condition interactions in somatosensory brain regions including right insula (b); Regions showing interaction effects corresponded with regions showing a decrease in activity during Diminish trials (relative to View) after the intervention in the Osc+ participants (c, left) but not with the occipital cluster showing a significant effect of time-point in Osc- participants (c, right). There were no effects of condition or time-point on ratings during Diminish trials (d); but for View trials, there was a significant interaction of condition and time-point (d). During Intensify trials, there was a main effect of time-point, with participants across conditions indicating stronger feelings in the post- than the pre-intervention scan (d).

As a manipulation check, we first confirmed that the emotional pictures affected brain activity in emotion-related regions (including the amygdala) during view trials during the pre-intervention session (see Supplementary Fig. 6). As outlined in a separate report[26], we also examined differences between diminishing and intensifying emotions at baseline and found that these two processes do not target the same set of emotion-related brain regions. When participants tried to diminish emotional reactions, they were more likely to reduce activity in brain regions important for interoception whereas when they tried to intensify emotional reactions, they were more likely to increase activity in other emotion-related brain regions. Thus, despite a linear effect of down-regulation, control, and up-regulation (i.e., diminish < view < intensify) in subjective emotional intensity, a different set of emotion-related brain regions are targeted by the two regulatory processes. Given these marked baseline differences in how diminishing and intensifying emotions affect activity in emotion-related brain regions, in our fMRI analyses we examined the effects of down-regulation (i.e., view > diminish) and up-regulation (i.e., intensify > view) separately.

We first used ROI-based analyses to examine amygdala activity during emotion regulation trials. At baseline, we found significantly increased left amygdala activity during intensify trials

compared with view trials, $t(83) = 3.53$, $p = 0.001$, $r = 0.39$ (M = 0.10, SE = 0.02 for intensify and M = 0.04, SE = 0.02 for view) for the left amygdala and $t(83) = 1.73$, $p = 0.09$, $r = 0.19$ (M = 0.06, SE = 0.02 for intensify and M = 0.04, SE = 0.02 for view) for the right amygdala. But there were no significant differences in amygdala activity between diminish and view trials, t(83) = 0.64, p = 0.53, r = 0.06 (M = 0.03, SE = 0.02 for diminish and M = 0.04, SE = 0.02 for view) for the left amygdala and t(83) = 1.18, p = 0.24, r = 0.12 (M = 0.02, SE = 0.02 for diminish and M = 0.04, SE = 0.02 for view) for the right amygdala. Next, we examined whether post-intervention change in amygdala activity during emotion regulation trials differed between conditions. Change in amygdala activity did not show significant differences between conditions for the two contrasts, $t(82) = 1.47$, $p = 0.15$, $r = 0.32$ for view > diminish and t(82) = 0.03, $p = 0.97$, $r = 0.01$ for intensify > view in the left amygdala and $t(82) = 0.49$, $p = 0.63$, $r = 0.11$ for view > diminish and $t(82) = -0.97$, $p = 0.34$, $r = -0.21$ for intensify > view in the right amygdala (see Supplementary Table 4 for details).

Next, we compared each participant's post- vs. pre-intervention whole-brain pattern of brain activity during the Intensify trials and during the Diminish trials. We used the View condition as a baseline comparison. There were no significant interactions of condition by time-point for the Intensify > View contrasts. However, for the View > Diminish comparison, there was a significant interaction of time-point and condition in clusters within the right insula, central opercular cortex, parietal operculum cortex, postcentral gyrus, supramarginal gyrus, and superior parietal lobule (Fig. 6b). Comparison of post versus pre time-points for each group indicated that these interactions were driven by the Osc+ group who improved their ability to diminish brain activity in many interoceptive/sensory regions relative to View after the intervention (Fig. 6c). The only significant change for this contrast in the Osc- group was in the occipital pole (Fig. 6c), but it was a cluster that did not overlap spatially with the condition-by-time-point interaction effect shown in Fig. 6b (see Supplementary Table 5 for the list of clusters).

Subjective ratings during the explicit regulation (diminish and intensify) trials were similar across the two intervention conditions and both groups rated pictures as more intense on Intensify trials after the intervention than before the intervention, $F(1, 81) = 9.03$, $p = .004$, $r = .32$ (Fig. 6d). However, when simply viewing pictures, there was an interaction of time-point and condition, $F(1,81) = 5.65$, $p = .02$, $r = .26$ (Fig. 6d). This interaction effect appeared to be due to both the Osc+ decrease, $p = 0.10$, and the Osc- increase, $p = 0.09$, in ratings of feeling strength during view trials after intervention, although the pairwise comparisons were not significant (see Supplementary Table 6 for details). Thus, although the interventions did not differentially influence conscious emotion regulation, they had differential effects on spontaneous responses to emotional pictures, potentially indicating changes in implicit emotion regulation[27]. Group differences in change may have emerged during the view but not regulation trials due to higher demand effects to give instruction-consistent responses during regulation trials than during view trials that constrained our ability to see change. Another possibility is that the effects of the intervention were stronger for implicit than for explicit emotion regulation processes[27], leading to decreased emotional responding during baseline view trials.

We also examined whether the daily biofeedback affected subjective well-being. Self-rated mood became less negative across the course of the intervention (Supplementary Fig. 7a), with no significant difference in change between conditions. Self-rated anxiety showed no significant changes nor condition differences (Supplementary Fig. 7b), while scores on a depression scale showed improvements across the intervention in both conditions (Supplementary Fig. 7c). Most previous studies examining the effects of heart rate variability biofeedback have relied on no-intervention controls[5]; our findings highlight the importance of equating factors other than the critical physiological manipulations across conditions, as factors in the active intervention other than changes in heart rate variability may have an impact. One such factor influencing subjective ratings could be expectations. For both groups we framed the study as testing whether their biofeedback intervention would improve

emotional well-being (e.g., Fig. 2a-b) and the two groups had similar expectations of improved well-being (Supplementary Fig. 2).

Discussion

Hundreds of previous studies have identified vagal HRV (usually assessed using HF-HRV or RMSSD) at rest as one of the best indicators of well-being[28-30]. In addition, individual differences in vagal HRV have been linked with brain structures and circuits associated with emotion regulation[3,20,31,32]. However, we need more than observational correlations to better understand the causal dynamics of the relationships. Initial studies do provide causal evidence that the prefrontal cortex influences vagal HRV, as perturbing PFC with either a drug blockade[33] or non-invasive brain stimulation[34,35] can influence HF-HRV. In addition, daily sessions involving increasing HRV through paced breathing and HRV-biofeedback have long-term effects on well-being[4,5,7,36], suggesting that, when it comes to the relationship between the brain and the heart, there are likely causal effects in both directions as suggested by Darwin about 150 years ago[37].

Our study followed up on these intriguing HRV-biofeedback effects on well-being to test the hypothesis that experiencing daily sessions involving increased heart rate oscillation (the Osc+ condition) would affect both resting-state functional connectivity within emotion networks as well as the responsiveness to emotion regulation attempts in brain regions involved in emotional experience. To increase the amplitude of heart rate oscillation, the Osc+ intervention involved slow paced breathing at approximately the frequency of the baroreflex to create resonance[7]. Previous findings indicate increases in heart rate oscillatory amplitude during resonance breathing are vagally mediated[22].

When planning this study, we selected changes in right amygdala-mPFC functional connectivity as our primary outcome measure because of our observation that right amygdala-mPFC functional connectivity was associated with HRV[20], and we were interested in whether HRV plays a causal role in increasing functional connectivity within this circuit. In the current study, spending 20-40 minutes/day

in a high physiological oscillatory state for a few weeks had no significant effect on right amygdala-mPFC connectivity, thus failing to confirm our main hypothesis. However, this intervention did increase left amygdala-mPFC functional connectivity. A prior meta-analysis identified the left (but not right) amygdala as showing activity related to HRV[3] and our prior study examining the relationship of how amygdala functional connectivity relates to individual differences in HRV found that, in younger adults, both left and right amygdala connectivity with ventrolateral PFC was related to HRV[20]. Thus, prior studies have identified both right and left amygdala relationships with HRV.

In a recent review, we proposed that daily time spent stimulating physiological oscillatory activity should increase chronic levels of oscillatory activity in emotion-related resting-state brain networks[4]. Indeed, our analyses examining the broader context of functional connectivity within canonical resting-state networks indicate that the functional connectivity changes seen in the left amygdala are not unique; instead they are part of a general pattern in our study of increased functional connectivity in emotion-related networks in the Osc+ condition, an increase in functional connectivity that is greater than in non-emotion networks.

One of our secondary outcomes examined whether the intervention would influence participants' ability to up- or down-regulate amygdala activity on demand. There were no significant effects of the intervention on amygdala activity during emotion regulation. However, when we examined whole-brain activity we found that the Osc+ intervention led to more effective down-regulation of brain regions associated with body states when attempting to regulate emotional responses to pictures.

Why would the intervention affect the ability to down-regulate brain regions associated with sensing somatic states but not the amygdala? There are different models of how cognitive appraisal (the strategy used by most participants in our study) affects amygdala activity. In one model, cognitive control regions (i.e., dorsolateral, ventrolateral and ventrolateral subregions of PFC and posterior

parietal cortex) engage ventromedial PFC (vmPFC), which via its anatomical connectivity with the amygdala relays the control messages[21]. This model guided our initial hypothesis that increased functional connectivity between mPFC and amygdala would increase Osc+ participants' ability to regulate amygdala activity. However, in another model, prefrontal and parietal control regions affect amygdala by altering semantic and perceptual representations in lateral temporal areas when reappraising stimuli[21]. Meta-analyses of emotion regulation studies support the latter model in which conscious reappraisal does not rely on vmPFC to influence amygdala activity[21,38]. Instead, the vmPFC may influence the amygdala more during implicit emotion regulation processes[20]. If the vmPFC is not engaged in the reappraisal process, this could explain how the Osc+ intervention could increase amygdala-mPFC functional connectivity during rest but not enhance modulation of amygdala activity during reappraisal.

Although decreases in amygdala activity during emotion down-regulation have been the most consistently documented outcome, in healthy participants, inferior parietal lobule activity also decreases during emotion down-regulation[39]. In addition, a meta-analysis revealed that, during reappraisal of negative stimuli, patients with mood and anxiety disorders show more activity in a set of brain regions that overlaps regions that Osc+ participants were better able to down-regulate after the intervention, including the right posterior insula, right inferior and superior parietal lobule, right postcentral gyrus, and right operculum[40]. These brain regions process signals from the body. Large oscillations in heart rate may strengthen feedback loops involving these brain regions, making these feedback loops more responsive during emotion regulation attempts and increasing participants' ability to down-regulate activity in these brain regions that not only sense body states, but also simulate them, such as when viewing pictures of others[17]. Our findings suggest that daily practice increasing heart rate oscillatory activity improved participants' ability to diminish activity in brain regions involved in feeling emotional body states when they wanted to minimize their emotional reactions to stimuli.

We also saw effects of the intervention on resting-state physiology. The Osc+ intervention increased heart rate oscillatory power in the resonance frequency range that participants had been breathing at during training, as reflected in increased LF-HRV at rest. Prior HRV-biofeedback studies consistently demonstrate acute changes in HRV during the training sessions, but evidence for long-term changes in HRV during rest has been more tenuous[41]. Our study had a larger N than prior HRV-biofeedback studies and also documented excellent adherence to the intervention, which in most prior studies was neither tracked nor rewarded (and so rates of home training in prior studies may have tended to be low).

The Osc+ intervention not only increased heart rate oscillatory activity at rest, but also BOLD oscillatory activity (ALFF) at rest, broadly across many brain networks. Thus, one possibility is that the ALFF changes stem from systemic neurovascular changes[42]. In contrast, the Osc+ intervention increased functional connectivity significantly only in networks related to emotion/interoception and not generally across all resting-state networks. Thus, it was specifically within brain networks that respond to and modulate fluctuations in physiology that within-network coordination of activity became stronger.

One of the unique strengths of our study compared to most previous HRV-biofeedback studies was the active comparison group (Osc-) who completed an intervention similar to the target Osc+ intervention, but with minimal effects on HRV (see Fig. 2). We found that participants in both conditions showed significant decreases in negative mood states and in depression scores. Thus, the active comparison group was important in revealing that some aspects of the biofeedback protocol other than its effects on HRV were associated with improved emotional well-being. One possibility is that spending time every day in an awake quiet restful state yields emotional benefits regardless of whether the relaxing state increases physiological oscillatory activity. Another is that participants' expectations (which were similarly positive in the two conditions) led to the improvements in self-

reported emotional states. It is also possible that the CES-D is not the best depression scale to assess HRV biofeedback effects[36]. In any case, these findings point to the importance of including active comparison groups with matched expectations in research examining the effects of behavioral interventions on well-being[43].

Across both conditions, more than half of the participants in our study were Asian. We recruited on campus; our Asian student overrepresentation may reflect ethnic differences in interest in participating in a study related to heart rate biofeedback and meditation. As Asians and European Americans differ in their ideal affect[44] and cardiovascular physiology differs between African Americans and European Americans[45], future studies should examine whether heart rate variability biofeedback effects differ by ethnicity.

In conclusion, we found that, in young healthy adults, daily sessions involving high amplitude heart rate oscillations affected emotion-related brain activity both when resting and when diminishing emotional responses. Repeated large heart-rate increases/decreases during biofeedback sessions provide a powerful physiological input that may act as a "workout" for cortical regions involved in physiological control, enhancing the brain's capacity to respond in goal-consistent ways when later confronted with emotional stimuli.

Methods

Participants

We recruited 121 participants aged between 18 and 35 years via the USC Healthy Minds community subject pool, a USC online bulletin board, Facebook and flyers (see Supplementary Fig. 1 for drop-out rates per condition; see the supplementary methods section for power considerations). Participants provided informed consent approved by the University of Southern California (USC) Institutional Review Board. Participants were assigned to small groups of 3-6 people, with each group meeting at the same time and day each week. After recruitment and scheduling of each wave of groups

were complete, groups were randomized to a condition. Upon completing the study, participants were paid for their participation and received bonus payments based on their individual and group performances (incentives for training were the same across conditions; see Supplementary Information for more details). Prospective participants were screened and excluded for major medical, neurological, or psychiatric illnesses. We excluded people who had a disorder that would impede performing the HRV biofeedback procedures (e.g., coronary artery disease, angina, cardiac pacemaker), who currently were training using a relaxation, biofeedback or breathing practice, or were on any psychoactive drugs other than antidepressants or anti-anxiety medications. We included people who were taking antidepressant or anti-anxiety medication and/or attending psychotherapy only if the treatment had been ongoing and unchanged for at least three months and no changes were anticipated. Gender, education, age and race were similar in the two conditions (Supplementary Tables 1 and 2).

Overview of 7-week Protocol Schedule

The study protocol involved seven weekly lab visits and five weeks of home biofeedback training (Fig. 1). Each lab visit began with questionnaires assessing mood and anxiety.

The first lab visit involved the non-MRI baseline measurements, including a number of questionnaires. The second lab visit involved the baseline MRI session followed by the first biofeedback training session. Each of the lab biofeedback training sessions started with a 5-min baseline rest period. The weekly lab visits (except for weeks with MRI sessions) were run in small groups in which participants shared their experiences and tips about biofeedback training with other participants from the same condition, while 1-2 researchers facilitated the discussion. Outside the lab, participants used a customized social app to communicate with other members of their group and researchers about their progress on daily biofeedback training. The Week 6 lab visit repeated the assessments from the first lab visit. The final (7^{th}) lab visit first repeated the baseline MRI session scans in the same order. Then,

additional training-session scans were collected at the end of the scan protocol. Finally, after the scan, participants completed a post-study questionnaire.

Biofeedback Training

Osc+ Condition. Participants wore an ear sensor to measure their pulse. They viewed real-time heart rate biofeedback while breathing in through the nose and out through the mouth in synchrony with a visual pacer. The software[46] provided a summary '**coherence**' score for participants that was calculated as peak power/(total power – peak power). Peak power was determined by finding the highest peak within the range of 0.04 – 0.26 Hz and calculating the integral of the window 0.015 Hz above and below this highest peak. Total power was computed for the 0.0033 – 0.4 Hz range.

During the second lab visit, we introduced participants to the device and had them complete five minutes of paced breathing at 6, 6.5, 5.5, 5 and finally 4.5 breaths/min[6]. Next, we computed various aspects of the oscillatory dynamics for each breathing pace using Kubios HRV Premium 3.1 software[47] and assessed which one had the most of the following characteristics: highest LF power, the highest maximum LF amplitude peak on the spectral graph, highest peak-to-trough amplitude, cleanest and highest-amplitude LF peak, highest coherence score and highest RMSSD. Participants were then instructed to train at home with the pacer set to this frequency that appeared to best approximate their resonance frequency and to try to maximize their coherence scores.

During the third visit, they were asked to complete three 5-min paced breathing segments: the best condition from the last week's visit, half breath per minute faster and half breath slower than the best condition. They were then instructed to train the following week at the pace that appeared most likely to be a resonance frequency based on the characteristics listed above. In subsequent weekly visits, during 5-min training segments, they were asked to try out abdominal breathing and inhaling through nose/exhaling through pursed lips as well as other strategies of their choice.

Osc- Condition. The same biofeedback ear sensor device was used in this condition. However, we created custom software to display a different set of feedback to the Osc- participants[48]. During each Osc- training session, a '**calmness**' score was provided as feedback to the participants instead of the coherence score. The calmness score was calculated by multiplying the coherence score that would have been displayed in the Osc+ condition by -1 and adding 10 (an 'anti-coherence' score). The net result was that participants got more positive feedback (higher calmness scores) when their heart rate oscillatory activity in the 0.04 – 0.26 Hz range was low.

We also wanted to avoid having participants figure out that one way to reduce their HRV and get positive feedback would be to do something like get up and do jumping jacks (physical activity typically decreases HRV[19]). Thus, we told Osc- participants to try to lower their heart rate in addition to lowering their heart rate oscillations and we intended to build into the feedback a minor point penalty when heart rate was the highest it had been in a short while. However, due to a coding error not detected until the study was over, this point adjustment did the opposite, giving a penalty when heart rate was the lowest it had been in the most recent 15 s. Specifically, every 5 s, a local maximum IBI was set based on the maximum IBI from the past 15 s. If, at that point, the participant's current IBI was longer than this local maximum, the calmness score displayed for the next 5 s was the anti-coherence score - 2. Naturally, most of the time, current IBI was lower than the local maximum, and in those cases, the calmness score was the anti-coherence score +1. Thus, there was a penalty in their calmness score for moments when their heart rate was slower than it had been in any of the past 15 s. As reported in the results, average heart rate during biofeedback sessions did not differ significantly across conditions. Thus, this additional feedback appeared to have had little impact on heart rate, consistent with prior findings that biofeedback to increase or decrease heart rate has no significant impact[49].

During the initial calibration session at the end of the second lab visit, each participant was introduced to the device and feedback and was asked to come up with five strategies to lower heart

rate and heart rate oscillations. The participant was asked to wear the ear sensor and view real-time heart rate biofeedback while they tried each strategy for five minutes. We analyzed the data in Kubios and identified the best strategy as the one that had the most of the following characteristics: lowest LF power, the minimum LF amplitude peak on the spectral graph, lowest peak trough amplitude, multiple and lowest-amplitude LF peak, highest calmness score and lowest RMSSD. Participants were then instructed to use this strategy to try to maximize their calmness scores in their home training sessions.

On the third visit, they were asked to select three strategies and try each out in a 5-min session. The strategy identified as best (based on the same characteristics used in the initial calibration session) was selected as the one to focus on during home training. In subsequent weekly visits, during 5-min training segments, they were again asked to try out strategies of their choice.

Post-Study Questionnaire

After the Week-7 post-intervention scan, participants completed a questionnaire surveying their experience during the study. They provided self-ratings of difficulty of daily heart rate biofeedback training, level of effort to complete the training, expectations of the training impact on well-being, and likelihood of continuing the training after the study's conclusion.

MRI Scan Session Order

In both the pre- and post-intervention MRI sessions, scans were conducted in the following order: 1) rest during blood oxygen level dependent (BOLD) fMRI; 2) rest during pseudo-continuous arterial spin labeling (pCASL); 3) emotion regulation task during fMRI; and 4) structural scan. The post-intervention session included an additional BOLD fMRI scan followed by a pCASL scan conducted after these four initial scans so as not to influence them. During these two additional training-mimicking post-intervention scans, participants engaged in their now-daily training practice (see below for details).

MRI Scan Parameters

We employed a 3T Siemens MAGNETOM Trio scanner with a 32-channel head array coil at the USC Dana and David Dornsife Neuroimaging Center. T1-weighted 3D structural MRI brain scans were acquired pre and post intervention using a magnetization prepared rapid acquisition gradient echo (MPRAGE) sequence with TR = 2300 ms, TE = 2.26 ms, slice thickness = 1.0 mm, flip angle = 9°, field of view = 256 mm, and voxel size = 1.0 x 1.0 x 1.0 mm, with 175 volumes collected (4:44 min). Functional MRI scans during the emotion-regulation task and resting-state scans were acquired using multi-echo-planar imaging sequence with TR= 2400 mm, TE 18/35/53 ms, slice thickness = 3.0 mm, flip angle = 75°, field of view = 240 mm, voxel size = 3.0 x 3.0 x 3.0 mm. We acquired 250 volumes (10 min) for the emotion-regulation task and 175 volumes (7 min) for the resting-state scans. PCASL scans were acquired with TR = 3880, TE = 36.48, slice thickness = 3.0 mm, flip angle = 120°, field of view = 240 mm and voxel size = 2.5 X 2.5 X 3.0 mm, with 12 volumes collected (3:14 min; 1st volume was an Mo image, 2nd volume was a dummy image, and the remaining 10 volumes were 5 tag-control pairs) both during resting-state (pre and post) and training-mimicking (post) scans. This ASL approach provides high precision and signal-to-noise properties and has better test-retest reliability than pulsed or continuous ASL techniques[50].

Pre- and Post-Intervention BOLD Resting-state Scan

Participants were instructed to rest, breathe as usual and look at the central white cross on the black screen.

Pre- and Post-Intervention pCASL Resting-state Scan

To assess whether the intervention affected blood flow during rest, in both MRI sessions participants completed a second short resting-state scan. Participants were instructed to rest while breathing normally with their eyes open. To make visual inputs similar to those viewed during the training scan (for our analyses comparing rest vs. training scans), we presented red and blue circles

alternately at a random rate (see *Training sessions during BOLD and pCASL* section below). Participants were asked not to pay attention to these stimuli.

Training-Mimicking Sessions During BOLD and pCASL

In the post-intervention scan session after the resting-state and emotion-regulation scans, participants completed their daily training without biofeedback during BOLD and pCASL scans. By this point, participants were well-trained, having each completed on average 57 training sessions at home. For the Osc+ group, a red and blue circle alternated at their resonance frequency. For example, if their resonance frequency was 12 sec, the red circle was presented for 6 sec followed by the blue circle for 6 sec. Participants were asked to breathe in with the red circle and breathe out with the blue circle. For the Osc- group, the stimuli were the same as the Osc+ group; however, the red and blue circles alternated at a random rate and participants were told not to pay attention to them.

Emotion Regulation Task

Participants completed an emotion regulation task[51] in the MRI scanner, which lasted for about 10 min. Each trial consisted of three parts: instruction (1s), regulation (6s), and rating (4s). First, participants were given one of three instructions: "view", "intensify," or "diminish." Then, during the regulation phase, they saw a positive, neutral or negative image. Finally, they were asked to rate the strength of the feeling they were experiencing on a scale ranging from 1 (very weak) to 4 (very strong).

Before the task, we instructed participants that the cue "intensify" would indicate they should escalate the emotion evoked by the subsequent image to feel the emotion more intensely. On the other hand, we instructed them that the cue "diminish" would indicate they should moderate the emotion elicited by the image in such a way that they felt calmer. We instructed them that the cue "view" meant they should simply look at the image without trying to change the emotion. We asked them to come up with their own methods to accomplish these emotion regulation goals. If participants had a hard time doing so during practice trials, we provided them with examples such as reinterpreting

the situations in the image and adjusting the distance between the objects in the picture and themselves. We also instructed them not to generate an emotion opposite to the one they were experiencing. For example, they were not supposed to substitute a positive emotion for a negative one to moderate their emotion. After MRI scans, we had participants rate their confidence in accomplishing the four emotion regulation conditions (e.g., diminish negative) and report their emotion regulation strategies.

Trials from each condition were nested in groups of three within mini-blocks. A fixation cross with a jittering interval separated the same-condition events within each block such that two jittering intervals summed up to 4s. The blocks were separated by 5-s inter-block intervals, during which a fixation cross was displayed. This resulted in 14 blocks and 42 event-related trials in total. The blocks were presented in a pseudo-random manner such that no blocks with identical instruction nor blocks with same-valence images were presented consecutively. We selected six counterbalanced sets of 18 positive, 18 negative, and 6 neutral images from the International Affective Picture System[52] such that within each of the six sets, each picture valence type subset had the same average valence and arousal scores (positive images: mean valence = 7.2, mean arousal = 5.4; negative images: mean valence = 2.8, mean arousal = 5.4; neutral images: mean valence = 5.0, mean arousal = 2.8). Each participant was presented with one of these sets during the task scan before training and a different set after training.

Weekly Questionnaires

During each lab visit, participants completed the profile of mood states (POMS[53]) and the state anxiety inventory (SAI[54]). We used the 40-item version of POMS. Participants reported how much each item reflected how they felt at the moment using a scale from 1 (not at all) to 5 (extremely). Total mood disturbance was calculated by subtracting positive-item totals from negative-item totals. A constant value (i.e. 100) was added to the total mood disturbance to eliminate negative scores. Higher scores indicate greater negative affect. The SAI measures state anxiety using 20 statements. Participants

indicated how they felt at the moment on a scale from 1 (not at all) to 4 (very much so). Scores range between 20 and 80 and higher scores indicate greater anxiety. We also administered the Center for Epidemiological Studies Depression Scale (CES-D[55]) in Weeks 1, 2, 6 and 7. Positive scores indicate greater symptoms of depression.

Rewards for Performance

In addition to receiving compensation of $15 per hour for each lab visit, participants were eligible to receive rewards based on individual and group performance. For individual performance rewards, each week participants had the opportunity to earn $2 for each instance (up to a maximum of 10) they exceeded their assigned target score (target scores were assigned each week, and were the average of the top 10 scores earned from the previous week's training sessions plus 0.3). Group performance rewards were earned when members of a participant's group completed a minimum of 80% of their assigned biofeedback training minutes. For example, if a participant completed 100% of their training, they received an additional $3 for each group member who also completed 100% of their training. If a participant completed 80% of their training, they received an additional $2 for each group member who also completed at least 80% of their training. Rewards were calculated weekly, and participants received weekly updates on their earnings at their lab visit.

Analyses

Heart Rate Oscillations During Training

We used Kubios HRV Premium 3.1[47] to compute autoregressive spectral power for each training session. Heart rate data from ear sensors failed to save for the first four participants in the Osc- condition because of technical issues with the first version of the Osc- biofeedback software, leaving 102 participants' data across the two conditions (5827 sessions). We averaged the autoregressive total spectral power from all training sessions for each participant. We excluded five outliers who on a box-and-whisker plot were above Q3 + 3 * the interquartile range on total power on pre-intervention rest

(N=3), post-intervention rest (N=1), or average training (N=1), leaving an N of 97 (N_{Osc+} = 52; N_{Osc-} = 45; see Fig. 2e-f). In addition, we extracted the summed power within the 0.063~0.125 Hz range for each participant (corresponding with 8-16s, a range encompassing breathing paces used by Osc+ participants) to obtain a measure of resonance frequency oscillatory activity during biofeedback. Before conducting statistical analyses, we log transformed the power values.

Heart Rate Oscillations During Seated Rest

We compared autoregressive spectral power during the baseline rest sessions (5-min sessions before lab training sessions) in the lab in Weeks 2 vs. 7 (Fig. 2g-h), using the same processing steps and outlier removals as detailed above for the training data.

Heart Rate Oscillations, Breathing Rate and End-Tidal CO2 During fMRI Scans

Both photoplethysmogram (PPG) and breathing data were collected using Biopac MP150 Data Acquisition System using MR-compatible sensors during resting-state and emotion regulation fMRI scans in Weeks 2 and 7. The breathing belt, TSD201 transducer, converted changes in chest circumference to electric voltage signal, which were then 0.05-1Hz bandpass-filtered, amplified with 10 times of gain, sampled at 10kHz using RSP100C. During analyses using MATLAB, the respiration signal was downsampled at 1kHz and smoothed, and two iterations of peak detection were performed to obtain an average breathing rate across each scan duration. The PPG data were collected using a Nonin Medical 8600FO Pulse Oximeter at 10kHz sampling rate and downsampled at 1kHz using MATLAB. PPG data were also analyzed using Kubios HRV Premium Version 3.1 to obtain the frequency value with peak power within the high frequency range (0.15-0.4 Hz). The central frequency of the HF component derived from autoregressive spectral analysis was used as an alternate estimate of the breathing rate[56]. Among participants who had both breathing belt and PPG estimates of breathing, these two estimates were significantly correlated, $r(52) = 0.95$, $p < 0.001$, $r(56) = 0.95$, $p < 0.001$, $r(44) = 0.97$, $p<0.001$, and $r(44) = 0.94$, $p<0.001$ for the pre- and post-intervention resting-state scans and the pre- and post-

intervention emotion regulation scans, respectively. Thus, for the subjects whose breathing belt respiration data were missing or not of good quality (N = 13 and N = 9 at pre- and post-intervention respectively for resting state, N = 10 and N = 6 at pre- and post-intervention respectively for emotion regulation, N = 4 for training-mimicking), we used the HF-HRV-derived estimate of their breathing rate. Breathing data with sudden signal drops without immediate recovery were categorized as poor quality data. For these poor quality cases, breathing rate was then substituted with HF-HRV-derived estimates or excluded if the estimates were not available. We also excluded breathing data we could not precisely synchronize with fMRI data due to failures of the scan start signal to record in the respiratory recordings. Breathing data was available for the analysis of breathing rate changes for 84 participants for resting state (N_{Osc+} = 43; N_{Osc-} = 41), 79 participants for emotion regulation (N_{Osc+} = 45; N_{Osc-} = 34), and 80 participants for training mimicking (N_{Osc+} = 42; N_{Osc-} = 38).

Exhaled carbon dioxide (CO2) levels were measured using Philips NM3 Monitor (Model 7900) with nasal cannula. The CO2 levels were fed to Biopac MP150 Data Acquisition System and sampled at 10kHz. After the CO2 data were shifted with a 9-second delay and downsampled to 1kHz, peak detection was performed at the end of each breath. A time series of detected peaks were used to calculate its mean and standard deviation of end-tidal CO2. CO2 data was available only for 73 participants (N_{Osc+} = 38; N_{Osc-} = 35) during resting state, 64 participants (N_{Osc+} = 34; N_{Osc-} = 30) during emotion regulation and 80 participants (N_{Osc+} = 41 ; N_{Osc-} = 39) during training mimicking. Of these, we categorized CO2 data as poor quality if they showed sudden signal drops or stayed too low mostly due to loosened cannulas. We excluded 27 participants (N_{Osc+} = 13; N_{Osc-} = 14) during resting state, 18 participants (N_{Osc+} = 10; N_{Osc-} = 9) during emotion regulation, 7 participants (N_{Osc+} = 3; N_{Osc-} = 4) during training mimicking. Thus, 46 participants (N_{Osc+} = 25; N_{Osc-} = 21) for resting state, 45 participants (N_{Osc+} = 25; N_{Osc-} = 20) for emotion regulation, and 73 participants (N_{Osc+} = 38; N_{Osc-} = 35) for training mimicking had CO2 data available for the analyses.

Heart Rate Variability Spectral Frequency Analyses of Resting-State Scan

The PPG data from the resting-state scan were downsampled at 1kHz using MATLAB. The downsampled PPG data were analyzed using Kubios HRV Premium Version 3.1 to obtain the autoregressive power spectrum density. We applied smoothness priors detrending (lambda=500, cut-off frequency .035 Hz) and selected the automatic-correction option for artifact correction. We visually checked the automatic peak detection results and, when occasionally necessary, manually deleted or corrected spurious detections or marked undetected peaks. We collected the total power and extracted the autoregressive power spectral density vector from individual output files to calculate the power within a frequency range (.063~.43 Hz) covering both slow (resonance) and more typical breathing rates.

For the analysis of spectral frequency power from heart rate data during the resting-state scan, among the same participants included in spectral analyses of resting-state scan who had PPG data (N_{Osc+} = 39, N_{Osc-} = 40), we excluded two outliers (N_{Osc-} = 2) who on a box-and-whisker plot showed total power changes from heart rate above Q3 + 3 * the interquartile range and four more outliers (N_{Osc+} = 3, N_{Osc-} = 1) who on a box-and-whisker plot showed power within the breathing frequency range above Q3 + 3 * the interquartile range, leaving an N of 73 (N_{Osc+} = 36 ; N_{Osc-} = 37).

fMRI Data

Preprocessing. To minimize the effects of motion and non-BOLD physiological effects, we employed multi-echo sequences during our fMRI scans. Previous work indicates that BOLD T2* signal is linearly dependent on echo time, whereas non-BOLD signal is not echo-time dependent[57]. Thus, multi-echo acquisitions allow uncoupling of BOLD signal from movement artifact and significantly improve accuracy of functional connectivity analyses[58], with between 2-3 times the level of reliability of typical single-echo scans[59]. We implemented a denoising pipeline using independent components analysis

(ICA) and echo-time dependence to distinguish BOLD fluctuations from non-BOLD artifacts including motion and physiology[60].

BOLD Spectral Analyses of Resting-State and Training Scans. After preprocessing by meICA, we performed additional preprocessing steps using FSL, Analysis of Functional NeuroImaging (AFNI), and custom code written in MATLAB[61]. The additional preprocessing steps consisted of: (1) temporal despiking; (2) linear detrending; (3) spatial smoothing (full width at half maximum [FWHM] = 6 mm) and (4) global intensity normalization. We converted the preprocessed images into ASCII files for processing by custom MATLAB code. To remove lower frequencies in the BOLD signal and investigate the band linked with respiratory oscillations, we applied smoothness priors detrending with parameter lambda = 4, which corresponds to the cutoff frequency 0.04 Hz[62]. We estimated voxel-wise power spectral density (PSD) using the autoregressive (AR) Burg method for each individual scan to capitalize on the improved accuracy of autoregressive approaches relative to the conventional fast Fourier[63]. To determine the model order, we first obtained estimates of the best model order using SPSS forecasting ARIMA's Bayesian information criterion (BIC), autocorrelation function (ACF) and partial-autocorrelation function (PACF) for each participant. Once the best model order for each individual was determined, the modal score across participants (model order = 3) was selected. After voxel-wise PSD estimation, the individual output files were converted into nifti files and the PSD map images were normalized to the MNI152 2-mm template using the transformation matrix from the individual preprocessed images. Whole brain average PSD vectors were extracted and power values were log transformed for the statistical analysis.

Amplitude of low frequency fluctuations (ALFF) analysis was performed on the obtained power spectrum using the autoregressive method. Since the power at a given frequency is proportional to the square of the amplitude at that frequency component, we calculated the square root of power at each frequency and obtained the averaged square root across the 0.–0.1 Hz frequency range at each voxel.

This averaged square root was our ALFF measure[64]. We applied 18 intrinsic connectivity network masks thresholded at 3.1 ($p < 0.001$) from Laird et al. (2011) on whole-brain ALFF images and we extracted average ALFF for each participant for each network at the pre- and post-intervention time-points. We calculated average values across the five emotion networks, four motor/visuospatial networks, three visual networks and six cognitive networks and computed the difference between post and pre functional connectivity values.

For the statistical analyses for the training scan (see Fig. 3b), we excluded seven participants; two people who failed to complete the scan due to time constraints ($N_{Osc+} = 1$, $N_{Osc-} = 1$), one person who failed to complete the scan due to feeling unwell ($N_{Osc+} = 1$), three people due to errors in stimulus presentation ($N_{Osc+} = 3$), and one participant due to unsuccessful results of the denoising pipeline ($N_{Osc-} = 1$). Additionally, we excluded six outliers ($N_{Osc+} = 2$, $N_{Osc-} = 4$) who on a box-and-whisker plot showed total power above Q3 + 3 * the interquartile range for their condition on the training scan, leaving an N of 87 ($N_{Osc+} = 45$, $N_{Osc-} = 42$). For the analyses comparing training scan and pre-intervention rest (see Fig. 3a), the 83 participants who were included for both the training scan and the pre-intervention resting-state scan were included ($N_{Osc+} = 43$, $N_{Osc-} = 40$). For the analysis comparing pre-intervention and post-intervention resting-state scans (see Fig. 2c), we excluded two participants ($N_{Osc+} = 1$, $N_{Osc-} = 1$) due to unsuccessful results of the denoising pipeline for their resting-state data and we excluded two outliers ($N_{Osc+} = 1$, $N_{Osc-} = 1$) who on a box-and-whisker plot showed total power changes above Q3 + 3 * the interquartile range. Additionally, we excluded two outliers ($N_{Osc+} = 2$) who on a box-and-whisker plot showed breathing rate changes above Q3 + 3 * the interquartile range or breathed at their own resonance frequency as if they were engaged in the Osc+ biofeedback, leaving an N of 94 ($N_{Osc+} = 48$; $N_{Osc-} = 46$).

Resting State Functional Connectivity. Seed-based functional connectivity analysis: Out of 100 participants who completed the resting state scan before and after the intervention, two

participants (one person from each condition) were excluded due to unsuccessful denoising pipeline results. Additionally, two Osc+ participants were excluded due to the fact that during the post-intervention resting state scan they breathed slowly as if they were engaged in the Osc+ biofeedback (see *BOLD spectral analyses of resting-state and training scans* section above). In the remaining 96 participants, we examined the resting-state functional connectivity between mPFC and amygdala. The mPFC was defined based on a previous meta-analysis of brain regions where activity correlated with HRV[3] (i.e., a sphere of 10mm around the peak voxel, x=2, y=46, z=6). The right and left amygdala were each anatomically defined using that participant's T1 image. The segmentation of the right and left amygdala was performed using the FreeSurfer software package version 6 using the longitudinal processing scheme implemented to incorporate the subject-wise correlation of longitudinal data into the processing stream (http://surfer.nmr.mgh.harvard.edu)[65]. Labels from the specific structures (left/right amygdala) were saved as two distinct binary masks in the native space. All files were visually inspected for segmentation accuracy at each time point. We used FSL FLIRT to linearly align each participant's preprocessed data to their brain-extracted structural image and the standard MNI 2-mm brain. We applied a low-pass temporal filter 0-0.1 Hz and extracted time series from the mPFC. For each participant, a multiple regression analysis was performed in FSL FEAT with nine regressors including the mPFC time series, signal from white matter, signal from cerebrospinal and six motion parameters. The individual amygdalae were registered to the standard MNI 2-mm brain using FSL FLIRT using trilinear interpolation followed by a threshold of 0.5 and binarise operation with fslmaths in order to keep the mask a similar size. From each participant's mPFC connectivity map, we extracted the mean beta values from the right and left amygdalae region-of-interests (ROIs) separately, which represents the strength of functional connectivity with mPFC. Lastly, we performed 2 (condition: Osc+, Osc-) × 2 (time point: pre, post) mixed ANOVAs on functional connectivity between mPFC and the left amygdala and between mPFC and the right amygdala.

Dual regression analysis: The same four participants were excluded as for the seed-based connectivity analysis. The six motion parameters and signal from white matter and cerebrospinal fluid were removed from each participant's preprocessed data. We used FSL FLIRT to linearly align the denoised data to each participant's brain-extracted structural image and the standard MNI 2-mm brain. A low-pass temporal filter 0-0.1 Hz was applied in order to remove high frequency fluctuation. These data were used in a FSL dual-regression analysis [66], in which we created subject-specific time series based on spatial maps for each of 18 canonical resting state networks from a prior study[67]. These individual time series were used to create subject-specific spatial maps of each network. From the subject-specific z-transformed spatial maps, we extracted mean functional connectivity values for each participant within an ROI of each of the corresponding canonical network using Laird et al's[67] network masks thresholded at 3.1 ($p < 0.001$). As done for ALFF values, we calculated average values within each network category (emotion/interoception, motor/visuospatial, visual, and cognitive) and computed the difference between post and pre functional connectivity values.

Arterial Spin Labeling. A total of 88 participants had available complete (i.e., pre- and post-intervention) pCASL data. Twenty-two participants were excluded due to errors in preprocessing or excessive motion, resulting in a total of 61 participants in subsequent pCASL analyses involving pre- and post- intervention scans, and a total of 53 participants in analyses involving pre-intervention and training scans. Data were preprocessed using the Arterial Spin Labeling Perfusion MRI Signal Processing Toolbox (ASLtbx)[68]. Mo calibration image and 10 tag-control pairs were motion corrected, co-registered to individual participants' T1-weighted structural images, smoothed with a 6 mm full width at half maximum Gaussian kernel, and normalized to MNI template space. Preprocessing resulted in a time-series of 5 perfusion images representing the tag-control pairs, which were averaged to create a single mean whole brain perfusion image.

We conducted voxel-wise analyses of whole brain perfusion maps in SPM12 to investigate the effects of training group and time-point on cerebral blood flow with a two-way ANOVA model. We included a study-specific grey matter mask comprised of averaged grey matter segmentations across participants' T1-weighted structural scans in all voxel-wise analyses to restrict analyses to grey matter cerebral blood flow, as ASL has lower power to detect white matter than grey matter perfusion signal[69]. An absolute threshold of 0.01 ml/100g/min was applied to remove background voxels and voxels with negative values. Following model estimation, we examined interactions of group and scan type (rest pre vs. post; rest pre vs. training), and within-group pre vs. post comparisons.

Emotion Regulation Data. Ninety-eight participants (N_{Osc+} = 52, N_{Osc-} = 46) completed the emotion regulation scan before and after the intervention. Six participants (N_{Osc+} = 3, N_{Osc-} = 3) were excluded due to unsuccessful denoising pipeline results. Two participants (N_{Osc+} = 1, N_{Osc-} = 1) were excluded because task timing files were not saved correctly. Six participants (N_{Osc+} = 3, N_{Osc-} = 3) were excluded as they failed to respond to 50% or more of the trials. Eighty-four participants remained for fMRI analysis (N_{Osc+} = 45, N_{Osc-} = 39). For the emotional intensity rating analysis, we excluded an additional three subjects (N_{Osc+} = 2, N_{Osc-} = 1) whose data were collected with a malfunctioning response button device and four participants (N_{Osc+} = 2, N_{Osc-} = 2) who answered with the same number for all the trials. However, we included the six participants (N_{Osc+} = 3, N_{Osc-} = 3) for whom the fMRI denoising process was not successful. For the rating analysis, we analyzed 83 participants' responses (N_{Osc+} = 44, N_{Osc-} = 39).

Denoised data were analyzed using FMRIB Software Library (FSL) version 6.0.3[70]. Three levels of analyses were performed: individual BOLD signal modeling, post-pre difference within each subject, and testing the difference between groups. For each individual's pre- and post-intervention scans, a standard general linear model estimated BOLD signal during the six seconds of emotion regulation during each trial (see Fig. 6) with seven regressors: diminish-negative, diminish-positive, intensify-

negative, intensify-positive, view-negative, view-positive, and view-neutral. Instruction and rating phases were not modeled. Intensify > view and view > diminish contrasts were conducted across positive and negative picture trials. This first-level analysis included spatial smoothing with 5-mm FWHM, motion correction (MCFLIRT)[70], and high-pass filtering with 60os cutoff. Using a 12-degree of freedom linear affine transformation, each participant's BOLD image was registered to a T1-weighted structural image (we registered each pre- vs. post-intervention BOLD image to the T1 image obtained in the same scan session), which was then registered to the MNI-152 T1 2mm brain image. In the second-level analysis, we used FSL's fixed effect model to estimate the post-pre difference within subjects while controlling for the mean effect. In the third-level analysis, we performed mixed-effect analyses to compare the post-pre differences in emotion regulation conditions between the two intervention groups using FSL's *Randomise* tool with 5,000 permutations and Threshold-Free Cluster Enhancement (TFCE) multiple comparison correction ($p < .05$)[71].

To test whether the intervention changed amygdala activity during emotion regulation, we extracted amygdala BOLD activity from the results of the above general linear model using FSL's featquery function with binary masks of the left and right amygdala (segmented through the same method used for the resting-state scan analysis and remapped to the standard MNI 2-mm brain). The extracted BOLD activity was used as the dependent variable in an independent-means *t*-test of post-pre change across conditions and in a dependent-means *t*-test comparing intensify - view vs. view - diminish differences in amygdala activity, with Benjamini-Hochberg correction.

Mixed ANOVA models were applied to test how emotion intensity ratings changed before and after intervention and how the change differed between conditions for each trial type (Diminish, View, and Intensify; 12 trials/trial type).

Questionnaires

For the POMS, SAI, and CES-D, we fit a series of linear mixed effects models using the packages lme4[72] and lmerTest[73] in R Version 3.6.2[74]. For each measure, we tested fixed effects of time-point, training condition, and their interaction. For random effects, we included a random intercept for each subject, which fit the data better for all measures than did random effects structures with intercepts at the subgroup level or for subjects nested within subgroups, as determined using likelihood ratio tests. Random effects structures including random slopes led either to unidentifiable models or singular model fits. All models were fitted using maximum likelihood. Significance of fixed effects was determined using *F* tests with Satterthwaite's approximation for degrees of freedom. For each measure, we performed post hoc comparisons of estimated marginal means of scores from week 1 with those from each successive week (2-7 for POMS and SAI; 2, 6 and 7 for CES-D) and applied a Bonferroni correction for multiple comparisons using the R package emmeans[75]. All available data for all 106 participants were included for these analyses.

Other Measures of Heart Rate Activity

We used Kubios HRV Premium Version 3.1 to compute heart rate, the standard heart rate variability measures of low frequency HRV (LF-HRV, 0.04-0.15 Hz), high frequency HRV (HF-HRV, 0.15-0.4 Hz) and root mean squared successive difference (RMSSD) for baseline and training sessions during each lab visit. We fit separate models for heart rate, RMSSD, LF power and HF power, specifying fixed effects of time-point, training condition, and their interaction. Only data from weeks 2 and 7 were included in the statistical models to examine how each measure changed from pre- to post-training (and only baseline data from weeks 2 and 7 were included in the comparison of spectral power shown in Fig. 2g-h). Otherwise, we followed the same linear effect modeling set-up for these analyses as for the questionnaire data (see *Questionnaires* section above), using all available data for all 106 participants.

Data availability

Data supporting the findings of this study will be made publicly available at OpenNeuro.

Code availability

Source code for biofeedback to decrease HRV is available at

https://github.com/EmotionCognitionLab/emWave_HRV.

References

1 Balzarotti, S., Biassoni, F., Colombo, B. & Ciceri, M. Cardiac vagal control as a marker of emotion regulation in healthy adults: A review. *Biol. Psychol.* **130,** 54-66 (2017).

2 Holzman, J. B. & Bridgett, D. J. Heart rate variability indices as bio-markers of top-down self-regulatory mechanisms: A meta-analytic review. *Neurosci. Biobehav. Rev.* **74,** 233-255 (2017).

3 Thayer, J. F., Åhs, F., Fredrikson, M., Sollers, J. J. & Wager, T. D. A meta-analysis of heart rate variability and neuroimaging studies: implications for heart rate variability as a marker of stress and health. *Neurosci. Biobehav. Rev.* **36,** 747-756 (2012).

4 Mather, M. & Thayer, J. F. How heart rate variability affects emotion regulation brain networks. *Current opinion in behavioral sciences* **19,** 98-104 (2018).

5 Goessl, V., Curtiss, J. & Hofmann, S. The effect of heart rate variability biofeedback training on stress and anxiety: a meta-analysis. *Psychol. Med.*, 1-9 (2017).

6 Lehrer, P. *et al.* Protocol for heart rate variability biofeedback training. *Biofeedback* **41,** 98-109 (2013).

7 Lehrer, P. M. & Gevirtz, R. Heart rate variability biofeedback: how and why does it work? *Frontiers in psychology* **5,** 756 (2014).

8 Lehrer, P., Sasaki, Y. & Saito, Y. Zazen and cardiac variability. *Psychosom. Med.* **61,** 812-821 (1999).

9 Peng, C. K. *et al.* Exaggerated heart rate oscillations during two meditation techniques. *Int. J. Cardiol.* **70,** 101-107 (1999).

10 Peng, C. K. *et al.* Heart rate dynamics during three forms of meditation. *Int. J. Cardiol.* **95,** 19-27, doi:http://dx.doi.org/10.1016/j.ijcard.2003.02.006 (2004).

11 Bernardi, L. *et al.* Effect of rosary prayer and yoga mantras on autonomic cardiovascular rhythms: comparative study. *BMJ* **323,** 1446-1449, doi:10.1136/bmj.323.7327.1446 (2001).

12 Hagemann, D., Waldstein, S. R. & Thayer, J. F. Central and autonomic nervous system integration in emotion. *Brain Cogn.* **52,** 79-87 (2003).

13 Poppa, T. & Bechara, A. The somatic marker hypothesis: revisiting the role of the 'body-loop'in decision-making. *Current opinion in behavioral sciences* **19,** 61-66 (2018).

14 Smith, R., Thayer, J. F., Khalsa, S. S. & Lane, R. D. The hierarchical basis of neurovisceral integration. *Neurosci. Biobehav. Rev.* **75,** 274-296 (2017).

15 Damasio, A. & Carvalho, G. B. The nature of feelings: evolutionary and neurobiological origins. *Nature Reviews Neuroscience* **14,** 143 (2013).

16 Bechara, A. & Damasio, A. R. The somatic marker hypothesis: A neural theory of economic decision. *Game Econ Behav* **52,** 336-372 (2005).

17 Keysers, C., Kaas, J. H. & Gazzola, V. Somatosensation in social perception. *Nature Reviews Neuroscience* **11,** 417-428 (2010).

18 Terathongkum, S. & Pickler, R. H. Relationships among heart rate variability, hypertension, and relaxation techniques. *J. Vasc. Nurs.* **22,** 78-82 (2004).

19 Sarmiento, S. *et al.* Heart rate variability during high-intensity exercise. *Journal of Systems Science and Complexity* **26,** 104-116 (2013).

20 Sakaki, M. *et al.* Heart rate variability is associated with amygdala functional connectivity with MPFC across younger and older adults. *Neuroimage* **139,** 44-52 (2016).

21 Buhle, J. T. *et al.* Cognitive reappraisal of emotion: a meta-analysis of human neuroimaging studies. *Cereb. Cortex* **24,** 2981-2990 (2014).

22 Kromenacker, B. W., Sanova, A. A., Marcus, F. I., Allen, J. J. & Lane, R. D. Vagal mediation of low-frequency heart rate variability during slow yogic breathing. *Psychosom. Med.* **80,** 581-587 (2018).

23 Reyes del Paso, G. A., Langewitz, W., Mulder, L. J., Roon, A. & Duschek, S. The utility of low frequency heart rate variability as an index of sympathetic cardiac tone: a review with emphasis on a reanalysis of previous studies. *Psychophysiology* **50,** 477-487 (2013).

24 Banks, S. J., Eddy, K. T., Angstadt, M., Nathan, P. J. & Phan, K. L. Amygdala–frontal connectivity during emotion regulation. *Social cognitive and affective neuroscience* **2,** 303-312 (2007).

25 Lee, H., Heller, A. S., Van Reekum, C. M., Nelson, B. & Davidson, R. J. Amygdala–prefrontal coupling underlies individual differences in emotion regulation. *Neuroimage* **62,** 1575-1581 (2012).

26 Min, J. *et al.* Emotion Down- and Up-Regulation Act on Spatially Distinct Brain Areas: Interoceptive Regions to Calm Down and Other Affective Regions to Amp Up. *bioRxiv* https://biorxiv.org/cgi/content/short/2021.09.20.461138v1 (2021).

27 Braunstein, L. M., Gross, J. J. & Ochsner, K. N. Explicit and implicit emotion regulation: a multi-level framework. *Social cognitive and affective neuroscience* **12,** 1545-1557 (2017).

28 Beauchaine, T. P. & Thayer, J. F. Heart rate variability as a transdiagnostic biomarker of psychopathology. *Int. J. Psychophysiol.* **98,** 338-350 (2015).

29 Geisler, F. C., Vennewald, N., Kubiak, T. & Weber, H. The impact of heart rate variability on subjective well-being is mediated by emotion regulation. *Pers. Indv. Diffs.* **49,** 723-728 (2010).

30 Kemp, A. H. & Quintana, D. S. The relationship between mental and physical health: Insights from the study of heart rate variability. *Int. J. Psychophysiol.* **89,** 288-296, doi:https://doi.org/10.1016/j.ijpsycho.2013.06.018 (2013).

31 Koenig, J. *et al.* Cortical Thickness and Resting State Cardiac Function Across the Lifespan: A Cross-Sectional Pooled Mega Analysis. *Psychophysiology* (2020).

32 Yoo, H. J. *et al.* Brain structural concomitants of resting state heart rate variability in the young and old: Evidence from two independent samples. *Brain Struct. Funct.* **223,** 727-737 (2018).

33 Ahern, G. L. *et al.* Heart rate and heart rate variability changes in the intracarotid sodium amobarbital test. *Epilepsia* **42,** 912-921 (2001).

34 Makovac, E., Thayer, J. F. & Ottaviani, C. A meta-analysis of non-invasive brain stimulation and autonomic functioning: Implications for brain-heart pathways to cardiovascular disease. *Neurosci. Biobehav. Rev.* **74,** 330-341 (2017).

35 Nikolin, S., Boonstra, T. W., Loo, C. K. & Martin, D. Combined effect of prefrontal transcranial direct current stimulation and a working memory task on heart rate variability. *PloS one* **12** (2017).

36 Pizzoli, S. F. *et al.* A meta-analysis on heart rate variability biofeedback and depressive symptoms. *Sci Rep* **11,** 1-10 (2021).

37 Darwin, C. (New York: Penguin, 1872).

38 Berboth, S. & Morawetz, C. Amygdala-prefrontal connectivity during emotion regulation: A meta-analysis of psychophysiological interactions. *Neuropsychologia* **153,** 107767 (2021).

39 Frank, D. *et al.* Emotion regulation: quantitative meta-analysis of functional activation and deactivation. *Neurosci. Biobehav. Rev.* **45,** 202-211 (2014).

40 Picó-Pérez, M., Radua, J., Steward, T., Menchón, J. M. & Soriano-Mas, C. Emotion regulation in mood and anxiety disorders: a meta-analysis of fMRI cognitive reappraisal studies. *Prog. Neuropsychopharmacol. Biol. Psychiatry* **79,** 96-104 (2017).

41 Wheat, A. L. & Larkin, K. T. Biofeedback of heart rate variability and related physiology: A critical review. *Appl. Psychophysiol. Biofeedback* **35,** 229-242 (2010).

42 Di, X., Kannurpatti, S. S., Rypma, B. & Biswal, B. B. Calibrating BOLD fMRI Activations with Neurovascular and Anatomical Constraints. *Cereb. Cortex* **23,** 255-263, doi:10.1093/cercor/bhs001 (2012).

43 Davidson, R. J. & Kaszniak, A. W. Conceptual and methodological issues in research on mindfulness and meditation. *Am. Psychol.* **70,** 581 (2015).

44 Tsai, J. L., Knutson, B. & Fung, H. H. Cultural variation in affect valuation. *J. Pers. Soc. Psychol.* **90,** 288 (2006).

45 Brownlow, B. N. *et al.* Ethnic Differences in Resting Total Peripheral Resistance: A Systematic Review and Meta-Analysis. *Psychosom. Med.* (2020).

46 EmWave Pro Plus (2016).

47 Tarvainen, M. P., Niskanen, J.-P., Lipponen, J. A., Ranta-Aho, P. O. & Karjalainen, P. A. Kubios HRV–heart rate variability analysis software. *Comput. Methods Programs Biomed.* **113,** 210-220 (2014).

48 Feng, T. *Biofeedback to decrease HRV* <https://github.com/EmotionCognitionLab/emWave_HRV> (2018).

49 Bennett, D. H., Holmes, D. S. & Frost, R. O. Effects of instructions, biofeedback, reward, and cognitive mediation on the control of heart rate and the application of that control in a stressful situation. *Journal of Research in Personality* **12,** 416-430 (1978).

50 Chen, Y., Wang, D. J. & Detre, J. A. Test–retest reliability of arterial spin labeling with common labeling strategies. *J. Magn. Reson. Imaging* **33,** 940-949 (2011).

51 Kim, S. H. & Hamann, S. Neural correlates of positive and negative emotion regulation. *J. Cogn. Neurosci.* **19,** 776-798 (2007).

52 Lang, P. J., Bradley, M. M. & Cuthbert, B. N. The international affective picture system (IAPS): Technical manual and affective ratings. (University of Florida, The Center for Research in Psychophysiology, Gainesville, FL, 1999).

53 Grove, J. R. & Prapavessis, H. Preliminary evidence for the reliability and validity of an abbreviated profile of mood states. *International Journal of Sport Psychology* (1992).

54 Spielberger, C. D. & Gorsuch, R. L. *Manual for the State-Trait Anxiety Inventory (Form Y) ("Self-Evaluation Questionnaire")* (Consulting Psychologists Press, 1983).

55 Radloff, L. S. The CES-D Scale: A self-report depression scale for research in the general population. *Applied Psychological Measurement* **1,** 385-401 (1977).

56 Thayer, J. F., Sollers, J. J., Ruiz-Padial, E. & Vila, J. Estimating respiratory frequency from autoregressive spectral analysis of heart period. *IEEE Eng. Med. Biol. Mag.* **21,** 41-45 (2002).

57 Kundu, P., Inati, S. J., Evans, J. W., Luh, W.-M. & Bandettini, P. A. Differentiating BOLD and non-BOLD signals in fMRI time series using multi-echo EPI. *Neuroimage* **60,** 1759-1770 (2012).

58 Dipasquale, O. *et al.* Comparing resting state fMRI de-noising approaches using multi-and single-echo acquisitions. *PloS one* **12** (2017).

59 Lynch, C. J. *et al.* Rapid precision functional mapping of individuals using multi-echo fMRI. *Cell reports* **33,** 108540 (2020).

60 Kundu, P. *et al.* Integrated strategy for improving functional connectivity mapping using multiecho fMRI. *Proceedings of the National Academy of Sciences* **110,** 16187-16192 (2013).

61 Biswal, B. B. *et al.* Toward discovery science of human brain function. *Proc. Natl. Acad. Sci. U. S. A.* **107,** 4734-4739, doi:10.1073/pnas.0911855107 (2010).

62 Tarvainen, M. P., Ranta-Aho, P. O. & Karjalainen, P. A. An advanced detrending method with application to HRV analysis. *IEEE Trans. Biomed. Eng.* **49,** 172-175 (2002).

63 Kay, S. M. & Marple, S. L. Spectrum analysis—a modern perspective. *Proceedings of the IEEE* **69,** 1380-1419 (1981).

64 Zou, Q.-H. *et al.* An improved approach to detection of amplitude of low-frequency fluctuation (ALFF) for resting-state fMRI: fractional ALFF. *J. Neurosci. Methods* **172,** 137-141 (2008).

65 Fischl, B. *et al.* Automatically parcellating the human cerebral cortex. *Cereb. Cortex* **14,** 11-22 (2004).

66 Nickerson, L. D., Smith, S. M., Öngür, D. & Beckmann, C. F. Using dual regression to investigate network shape and amplitude in functional connectivity analyses. *Frontiers in neuroscience* **11,** 115 (2017).

67 Laird, A. R. *et al*. Behavioral interpretations of intrinsic connectivity networks. *J. Cogn. Neurosci.* **23,** 4022-4037 (2011).

68 Wang, Z. *et al*. Empirical optimization of ASL data analysis using an ASL data processing toolbox: ASLtbx. *Magn. Reson. Imaging* **26,** 261-269 (2008).

69 van Osch, M. J. *et al*. Can arterial spin labeling detect white matter perfusion signal? *Magnetic Resonance in Medicine: An Official Journal of the International Society for Magnetic Resonance in Medicine* **62,** 165-173 (2009).

70 Jenkinson, M., Beckmann, C. F., Behrens, T. E., Woolrich, M. W. & Smith, S. M. Fsl. *Neuroimage* **62,** 782-790 (2012).

71 Smith, S. M. & Nichols, T. E. Threshold-free cluster enhancement: addressing problems of smoothing, threshold dependence and localisation in cluster inference. *Neuroimage* **44,** 83-98 (2009).

72 Bates, D., Mächler, M., Bolker, B. & Walker, S. Fitting linear mixed-effects models using lme4. *Journal of Statistical Software* **67,** doi:10.18637/jss.v067.i01 (2014).

73 Kuznetsova, A., Brockhoff, P. & Christensen, R. Tests in linear mixed effects models version. *Cran. URL https://cran. r-project. org/web/packages/lmerTest/lmerTest. pdf* (2016).

74 R: A language and environment for statistical computing. R Foundation for Statistical Computing (Vienna, Austria, 2019).

75 Searle, S. R., Speed, F. M. & Milliken, G. A. Population marginal means in the linear model: an alternative to least squares means. *The American Statistician* **34,** 216-221 (1980).

Acknowledgments

This study was supported by NIH R01AG057184 (PI Mather).

We thank our research assistants for their help with data collection: Michelle Wong, Kathryn Cassutt, Collin Amano, Yong Zhang, Paul Choi, Heekyung Rachael Kim, Seungyeon Lee, Alexandra Haydinger, Lauren Thompson, Gabriel Shih, Divya Suri, Sophia Ling, Akanksha Jain, and Linette Bagtas.

Authors' Information

These authors contributed equally: Kaoru Nashiro, Jungwon Min and Hyun Joo Yoo.

Contributions

K.N., J.M., and H.Y. equally contributed to the manuscript and are co-first authors. M.M. conceptualized the study, designed the study with the input from J.F.T., P.L., and C. Chang, and analyzed the data. K.N. helped design the study, directed the research team, collected and analyzed the data. J.M. and H.Y. helped with the initial setup and design of the study, collected and analyzed the data. Data collection was also performed by C. Cho with the assistance of S.L.B., P.N. and D.W. C. Cho, S.L.B. and S.D. also analyzed the data. J.F.T., P.L., C. Chang, D.A.N. and V.Z.M. provided technical assistance with data acquisition and analyses and helped interpret the results. With the supervision of S.N., T.F. developed a customized app for the Osc- training group and contributed to data management. N.M. developed a customized app for participants to track their training progress and contributed to data management. All authors contributed to manuscript preparation.

Competing Interests Statement

The authors declare no competing interests.